Journal of Medicinal Chemistry

Article

Design and synthesis of pyridone containing 3,4-dihydroisoquinoline-1(2H)-ones as a novel class of enhancer of zeste homolog 2 (EZH2) inhibitors

Pei-Pei Kung, Eugene Rui, Simon Bergqvist, Patrick Bingham, John Braganza, Michael R. Collins, Mei Cui, Wade Diehl, Dac M Dinh, Connie Fan, Valeria R. Fantin, Hovhannes J. Gukasyan, Wenyue Hu, Buwen Huang, Susan Kephart, Cody T Krivacic, Robert A. Kumpf, Gary Li, Karen A. Maegley, Indrawan McAlpine, Lisa Nguyen, Sacha Ninkovic, Martha A. Ornelas, Michael Ryskin, Stephanie Scales, Scott C. Sutton, John H Tatlock, Dominique Verhelle, Fen Wang, Peter A Wells, Martin Wythes, Shinji Yamazaki, Brian Yip, Xiu Yu, Luke Zehnder, Wei-Guo Zhang, Robert A. Rollins, and Martin P. Edwards

J. Med. Chem., **Just Accepted Manuscript** • Publication Date (Web): 11 Aug 2016

ACS Publications

Journal of Medicinal Chemistry is published by the American Chemical Society. 1155 Sixteenth Street N.W., Washington, DC 20036

	Yu, Xiu; Pfizer Global Research and Development La Jolla Zehnder, Luke; Pfizer Global Research and Development La Jolla Zhang, Wei-Guo; Pfizer Global Research and Development Rollins, Robert; Pfizer Inc, Oncology Edwards, Martin; Pfizer Global Research and Development La Jolla

Design and synthesis of pyridone containing 3,4-dihydroisoquinoline-1(2H)-ones as a novel class of enhancer of zeste homolog 2 (EZH2) inhibitors

Pei-Pei Kung[a]*, Eugene Rui[a], Simon Bergqvist[b], Patrick Bingham[b], John Braganza[a], Michael Collins[a], Mei Cui[b,^], Wade Diehl[a], Dac Dinh[b], Connie Fan[b], Valeria R. Fantin[b], Hovhannes J. Gukasyan[d], Wenyue Hu[e], Buwen Huang[a], Susan Kephart[a], Cody Krivacic[b], Robert A. Kumpf[a], Gary Li[b], Karen A. Maegley[b], Indrawan McAlpine[a], Lisa Nguyen[b], Sacha Ninkovic[a], Martha Ornelas[a], Michael Ryskin[b†], Stephanie Scales[a], Scott Sutton[a], John Tatlock[a], Dominique Verhelle[b], Fen Wang[a], Peter Wells[b], Martin Wythes[a], Shinji Yamazaki[c], Brian Yip[b], Xiu Yu[a], Luke Zehnder[a], Wei-Guo Zhang[b†], Robert A. Rollins[b†], and Martin Edwards[a]

[a]Oncology Chemistry; [b]Oncology Research Unit; [c]Pharmacokinetics, Dynamics, and Metabolism; [d]Pharmaceutical Science Research Enabling Group; [e]Drug Safety Research and Development;

Pfizer Global Research and Development, La Jolla Laboratories, 10770 Science Center Dr., San Diego, CA 92121, USA

[†]Pfizer Global Research and Development, 401 N. Middletown Rd., Pearl River, NY 10965, USA

[^]Mei Cui passed away on April 11, 2015.

Abstract. A new enhancer of zeste homolog 2 (EZH2) inhibitor series, comprised of a substituted phenyl ring joined to a dimethylpyridone moiety via an amide linkage, has been designed. A preferential amide torsion was identified for this series via computational analysis that improved the binding properties of the compounds. Cyclization of the amide linker resulted in a six member lactam analog, compound **18**. This transformation significantly improved the ligand efficiency/potency of the cyclized compound relative to its acyclic analog. Additional optimization of the lactam-containing EZH2 inhibitors focused on lipophilic efficiency (LipE) improvement which provided compound **31.** Compound **31** displayed improved LipE and on-target potency in both biochemical and cellular readouts relative to compound **18**. Inhibitor **31** also displayed robust in vivo anti-tumor growth activity and dose-dependent de-repression of EZH2 target genes.

INTRODUCTION

Epigenetic information is contained in living cells in many different forms that include DNA and histone modifications, nucleosome positioning, and microRNA expression.[1,2,3] Epigenetic dysregulation is a hallmark of many different cancer types, including both hematological malignancies and solid tumors.[4a,b] Among possible histone modifications, lysine methylation has gained increased attention due to the potential of the modified chromatin structures to regulate gene transcription, DNA replication, and DNA repair.[5] This epigenetic modification is controlled by families of methyltransferase and demethylase enzymes that coordinate the addition and removal of methyl groups to histone tails.[6] The aberrant activity of these epigenetic regulators in diseases such as cancer has made them attractive targets for the development of novel cancer therapies.[7a,b,c]

The histone methyltransferase enhancer of zeste homolog 2 (EZH2) is the catalytic subunit of the polycomb repressor complex 2 (PRC2).[8] The PRC2 complex has been shown to initiate long-term gene silencing by methylating lysine 27 on histone H3 (H3K27).[9] Activating point mutations, such as Y641N, Y641F, A677G, and A687V, in the catalytic SET (Su[var]3-9, enhancer of zeste, trithorax) domain of EZH2 are responsible for the elevated H3K27Me3 levels in diffuse large B-cell lymphoma (DLBCL) and follicular lymphoma (FL).[10-14] In addition, several selective EZH2 inhibitors have been shown to effectively kill lymphoma cells bearing these mutations, demonstrating that EZH2 enzymatic activity and elevated H3K27Me3 level are required for cell proliferation and survival in this setting.[14-18] In addition to EZH2-mutant lymphomas, small molecule inhibitors of EZH2 have also been reported to inhibit the proliferation of tumors that harbor wild type EZH2 but which also contain different somatic

mutations in subunits of the chromatin remodeling complex.[19] These specific mutations in the switch/sucrose nonfermentable (SWI/SNF) chromatin remodeling complex are SNF5/INI-1/SMARCB1 in malignant rhabdoid and synovial sarcoma[20,21] and ARID1A in ovarian cancer[22]. These observations stimulated numerous EZH2 drug discovery programs, and the first examples of such inhibitors have entered clinical trials for the treatment of diffuse large B-cell lymphoma (DLBCL), follicular lymphoma (FL), and SNF5/INI-1/SMARCB1 genetically defined solid tumors.

RESULT AND DISCUSSION

Our internal EZH2 inhibitor research program sought to identify small molecules that blocked the enzyme's SET domain catalytic function and therefore inhibited the formation of trimethylated H3K27. EZH2 inhibitors reported in the literature typically contain a pyridone moiety attached via an amide linkage to a bicyclic hetero-aryl group [Figure 1, **1** (GSK-126)[14], **2** (UNC-1999)[16], **3** (EI1)[17], **4** (CPI-169)[18]]. Unfortunately, the relatively large number of planar aromatic rings contained in such structures tends to impair the solubility of the resulting compounds.[23] One notable exception is **5** (EPZ-6438, Tazemetostat) which incorporates a phenyl ring in place of the bicylic group. This compound demonstrated impressive clinical response and has currently progressed to phase II trials with a recommended dose of 800 mg, twice a day (BID).[24] We were interested in identifying potent EZH2 inhibitors bearing a central phenyl ring that were structurally distinct to those previously reported. We envisioned that the new molecules might combine good solubility with favorable pharmacokinetic properties.[25]

We began our lead finding effort by incorporating the dimethylpyridone substituent common to many potent EZH2 inhibitors into a library containing various substituted heteroaromatic/phenyl/heterocyclic carboxyamides (Figure 2, total of 181 compounds, clogP

ranged from -1 to 3). One compound exhibited encouraging properties and afforded a measurable IC_{50} value in a lower-throughput biochemical assessment (compound **6**, Table 1). Accordingly, this compound was selected for additional modifications with the goal of further improving EZH2 inhibition potency.

As shown in Table 1, the di-substituted molecule **6** displayed improved EZH2 inhibition properties relative to the mono-substituted analogs **7** and **8** (Table 1). Encouragingly, inclusion of meta-ethoxy and meta-isopropoxy substituents in the inhibitor designs further improved inhibition potency (compounds **9** and **10**, Table 1). Interestingly, replacement of the ortho-methyl contained in **6** with a variety of other substituents, such as F, OCH_3, and OH, afforded compounds with significantly weaker EZH2 inhibition properties (compare **6** to **11**, **12**, and **13**). Of the additional ortho substituents investigated, only the Cl substituent retained acceptable EZH2 inhibition levels (compound **14**, Table 1). A similar trend was also observed with the meta-isopropoxy substituent (compared **10** to **15**, Table 1). These observations suggested that the torsional angle between the phenyl group and the amide carbonyl moiety plays an important role in EZH2 inhibition potency.

Small molecule crystal data from the Cambridge Crystallographic Database revealed a dependence of the torsion angle between the carbonyl and the phenyl ring as a function of the size and polarity of the R^1 substituent[26] (Figure 3). A regression analysis was performed using this distribution of conformational propensities and IC_{50} values for compounds **6, 8**, and **11**-**14**. This analysis indicated 50 ± 5 degrees as the optimal angle between the carbonyl and the phenyl ring. This single descriptor was able to explain 96% of the variance in binding affinity ($p<0.0001$) for this data set. The influence of this torsional angle on EZH2 inhibition can be rationalized by three non-exclusive hypotheses: (1) the linker orients the dimethyl pyridone and

phenyl rings into an optimal binding geometry, (2) the carbonyl oxygen makes an important hydrogen bond with a protein hydrogen bond donor that is located approximately 50 degrees above or below the plane of the phenyl ring, (3) the N-H of the amide linker makes an important hydrogen bond with a protein hydrogen bond acceptor that is located approximately 50 degrees above or below the plane of the phenyl ring.

To test these hypotheses, we explored rigidifying the inhibitor's conformation in the preferred binding mode as a means to improve EZH2 affinity. We initially employed a 7-membered lactam in the new inhibitor design since such inclusion maintained the critical amide torsion angle near the 50 degree optimum (compound **16**, Table 2) (see Table 1S in supplementary material for torsional angle analysis of the carbonyl moiety present in 7-membered lactam). Encouragingly, **16** exhibited dramatically improved EZH2 biochemical inhibition potency, roughly 50-fold relative to the un-cyclized compound **14** (Table 2). Importantly, this increased potency could not be simply ascribed to the improved binding through higher lipophilicity as LipE increased by about a unit as compared to **14**. This observation provided some encouragement for our cyclization strategy. Unfortunately, **16** was also highly unstable toward human liver microsomes and thus required additional optimization.

We next introduced an oxygen atom into the 7-membered lactam design with the expectation that lowering compound lipophilicity should favorably impact human liver microsome (HLM) stability. The resulting molecule (**17**, Table 2) exhibited improved HLM clearance properties but also lost some EZH2 inhibition potency relative to **16** though LipE minimally decreased (0.2). We next explored removing a methylene moiety from the lactam ring present in **16** as an alternate strategy to lower lipophilicity and improve HLM stability. The

resulting 6-membered lactam **18** displayed the desired improved HLM stability properties and exhibited EZH2 inhibition activity that was only slightly weaker than that exhibited by **16**.

Compounds **17** and **18** both displayed similar HLM clearance values (Table 2). However, **18** had a higher lipophilic metabolism efficiency (LipMetE)[27] value (0.36) compared with **17** (-0.27), suggesting that **17** contained an inherent metabolic soft spot. We therefore decided to focus additional optimization efforts on the 6-membered lactam inhibitor series. Accordingly, ethyoxy and isopropoxy substituents were used to replace the methoxy moiety present in **18**. The resulting compounds (**19** and **20**) displayed 3-10 fold potency improvement in the biochemical assay relative to **18**. Similar improvements were noted in the uncyclized benzamide series described earlier in this work (Table 1). However, in contrast to the Table 1 SAR, replacement of the Cl group present in **20** with a methyl substituent resulted in a 7-fold potency loss (compound **21**, Table 2). This difference may be due to subtle binding alterations between the cyclized and un-cyclized inhibitor series. In order to confirm the hypothesis of the importance of ortho substituents (such as Cl and Me) for the EZH2 inhibitory potency, compound **22** was synthesized, and this molecule lost significant potency relative to either compound **20** or **21**.

One notable feature of the 6-membered lactam inhibitor series is that the carbonyl torsion angle is calculated to be constrained to approximately 20° instead of the 50° optimum described above (Table 1S, supplementary material). In a comparison of matched compound pairs, the cyclized 6-membered lactam compounds exhibited consistently-improved biochemical potencies and LipE values relative to the corresponding un-cyclized analogs (Figure 4) suggesting a possible contradiction to the previous hypotheses regarding the carbonyl torsion angle. We suspect other binding improvements (for example: better contacts with the protein, and/or less

overall strain in the protein and/or ligand) associated with recognition of EZH2 by this 6-membered lactam series compensated for the less than ideal torsional angle in the 6-membered lactam inhibitor design.[28-30]

Enthalpy is a measure of changes in protonation state as well as the differential number and quality of interactions (hydrogen bonds, van der Waals, electrostatic, and strain contributions) between the protein, ligand, and solvent in the complex and unbound states. The previous stated hypotheses essentially relate to the enthalpy of binding. To gain insight into the EZH2 thermodynamic binding components, we performed isothermal titration calorimetry (ITC) studies on compound **21** and its un-cyclized analog **10**. As shown in Table 3, enthalpic contributions dominated the binding of both compounds to EZH2. However, the improved binding affinity of **21** was driven by an increase in favorable entropic contributions at the expense of a diminished enthalpic component relative to compound **10**.

There are numerous contributions to the energetic parameters determined from ITC experiments[31] and it is generally difficult to assign specific binding energy components to a particular functional group or residue.[32] The generally ubiquitous enthalpy-entropy compensation further hinders efforts at interpretation.[33] Therefore, while the loss in binding enthalpy for **21** relative to **10** is consistent with each of the three hypotheses regarding the carbonyl conformation, with currently available data[29] only hypotheses (1) and (2) appear to be candidates for explaining this difference.

Entropy differences arise from changes in solvent structure and residual mobility of the protein and ligand between bound and unbound states. It is tempting to attribute the changes in binding entropy to a greater rigidity for Compound **21** due to cyclization; however, as revealed by data in Figure 3, the exocyclic bond to the carbonyl is already conformationally biased in the

acyclic analog. This observation is consistent with calculations that estimate that the maximum differential conformational entropy contribution to be on the order of 0.14 kcal mol^{-1}. Compound **21**, with two additional methylenes and one less NH than **10,** is more lipophilic than compound **10** as evidenced by the difference in logD at pH 7.4 of 0.8 log units. However, as has been previously pointed out, a direct linkage between hydrophobicity and entropy cannot be established since many complexities exist.[34]

Compound **20** displayed reasonable biochemical WT and mutant Y641N potency, moderate HLM clearance (53.8 μL/min/mg), and permeability[35] (19.6 $x10^{-6}$ cm/sec). However, the cellular IC_{50} values of compound **20** associated with inhibiting H3K27Me3 and reducing cell proliferation were about 1 μM (Table 4). In order to utilize this novel class of EZH2 inhibitors in *in vivo* studies, we sought to further improve the compound's cell potency and biochemical lipophilic efficiency (LipE)[36a,b].

Toward this end, the isopropoxy moiety of compound **20** was selected as a site for further exploration. A small array of 30 compounds which contained various alkoxy groups that replaced the isopropoxy moiety present in **20** was designed and synthesized. Among these 30 molecules, compound **23**, which contained a chiral THF moiety and thus possessed reduced lipophilicity relative to **20**, maintained similar biochemical potency and improved LipE by about 1.5 units (calculated based on Y641N IC_{50}; Figure 5). Consequently, **23** displayed an improved HLM clearance value relative to **20** and also maintained good permeability (Table 5). In order to further improve the lipophilic efficiency of **23** binding to EZH2, other positions on its phenyl moiety were also modified. These efforts led to the R^4 position of the phenyl moiety being identified as a promising vector. In order to maintain the desired high ligand binding efficiency, small groups, such as F, CH_3, and Cl, were introduced as new R^4 substituents (compounds **24-26**,

Table 4). Compound **24**, which contains a fluorine atom at the R^4 position, lost about two-fold potency in both biochemical and cellular assays relative to inhibitor **23**. However, compound **25**, containing a CH_3 group at the R^4 position, improved potency by two fold and thus maintained similar LipE compared with **23** (Figure 5). Since compound **24** and **25** exhibited similar measured logD values, the latter molecule displayed a higher LipE value (about 0.5 units, Figure 5). This result indicated that R^4CH_3 was a better moiety to increase compound binding affinity relative to the R^4F substituent employed in **24**. Encouragingly, substituting the H atom at R^4 with Cl resulted in compound **26** which displayed about 5-fold and 3-fold potency improvements relative to **23** and **25**, respectively. Compounds **23**, **25**, and **26** displayed similar LipE values due to the increased lipophiliciy of **26** relative to **23** and **25** (Table 4 and Figure 5). Compound **26** was also about 3 to 5-fold more potent in reducing cellular H3K27Me3 levels and cell proliferation compared with **23**.

Compounds **26** and **23** displayed similar HLM clearance and permeability values (Table 5). However, **26** displayed lower kinetic solubility[37] compared with **23** (Table 5). Mouse PK data were collected on compounds **23** and **26**. Unfortunately, mouse PK experiments indicated that neither compound could afford free plasma exposures in excess of the corresponding cell IC_{90} values for at least 6 hours following a 300 mg/kg orally administrated dose (data not shown). As studies of other EZH2 inhibitors reported in the literature[15] suggested that such coverage was required to achieve in vivo efficacy, we sought to further improve both H3K27Me3 reduction and anti-proliferation parameters (target cell IC_{50} = 20 nM for reducing both cellular H3K27Me3 level and viability). Therefore, our optimization efforts continued via exploring more diverse chemical moieties attached to the R^2 position of the lactam scaffold.

We decided to include heteroaryl moieties at the R^2 position since they would probe a very different chemical space compared with the alkoxy groups. We initially chose to employ pyrazole moieties in this exploration since the pyrazole is a versatile heterocycle that could be further derivatized *via* the nitrogen atom if desired. As shown in Table 4, attachment of a substituted pyrazole via the 4-position to the inhibitor core afforded a compound (**27**, Table 4) that exhibited WT and Y641N IC_{50}s of 51 nM and 271 nM, respectively. Addition of a methyl group to the pyrazole 5-position improved inhibition potency by about 2 fold (compared **28** with **27**, Table 4) while incorporation of a second methyl group (compound **29**, Table 4) further enhanced the biochemical activity by 3-4 fold relative to **27**. Compounds **27**-**29** increased the associated lipophilicity relative to **26** (Table 4), but did not improve binding affinity. We next attempted to elaborate compound **29** by alkylating the pyrazole NH present in its structure. However, this modification was not tolerated (compound **30**) suggesting either that the NH was involved in an H-bonding interaction with the EZH2 protein and/or that the additional steric bulk could not be accommodated in the protein's binding site. To help differentiate these possibilities, we prepared the corresponding dimethyl-substitued isoxazole compound **31** (Table 4). Encouragingly, this molecule displayed very potent EZH2 biochemical inhibition as well as good activity in the cell H3K27Me3 reduction and anti-proliferation effect. Compound **31** displayed about 5-10 fold biochemical potency improvement relative to **26** and also increased logD by 0.5 units (Table 4). These changes collectively resulted in **26** and **31** exhibiting similar LipE values (Figure 5). Consistent with the SAR developed using R^2 alkoxy substituents, removal of the 4-Cl substituent from compound **31** resulted in a 4-fold loss in inhibition activity (compound **32**, Table 4). We were encouraged that compound **31** exhibited > 10-fold improvement in cell potency relative to **26** which maintaining similar biochemical LipE. We

therefore profiled **31** in several additional *in vitro* experiments to better understand its biological properties.

Compound **31** displayed biochemical and cellular potency in the Karpas-422 cell line that was comparable to other reported EZH2 inhibitors.[14-18] The compound was also shown to be competitive with the SAM substrate (Figure 1S, supplementary material) and thus displayed a mechanism of inhibition that was similar to other reported EZH2 compounds[14-18] Given the observation that EZH2 activity needs to be strongly inhibited for extended duration to improve efficacy in animals, an inhibitor with a long residence time would be advantageous. Unfortunately, traditional methods for measuring compound off-rates including jump dilution and surface plasmon resonance (SPR) could not be applied to compound **31**. Robust SPR methods have not been developed due to the large size of the complex as well as the potential for instability of the complex under continuous flow conditions. The jump dilution experiment is difficult to perform properly with tight binding inhibitors[38] and we were unable to use this method. Therefore, we developed a method that measures the enzyme bound compound directly by mass spectrometry (experimental methods and Figure 2S, supplemental material) following separation from free compound. Using this method we were able to observe an off-rate for compound **1** that is similar to the published value[39]. Comparison of the off-rates for **1**, compounds **31** and **32** (Table 2S, supplementary material) suggests that both compounds **31** and **32** have residence times which are at least comparable to, and potentially superior to compound **1**. Compound **31** was also profiled in the CEREP histone methyltransferase selectivity panel and Invitrogen kinase selectivity panel and was proven to be selective (Table 3S, supplementary material). To provide further proof of cellular target modulation as well as additional downstream biomarkers, compound **31** was tested for its ability to modulate the expression of

TNFRSF21 and PRDM1, two PRC2 target genes that have previously been shown to be repressed by H3K27Me3.[14,40] Upon treatment with compound **31** for 7 days, both TNFRSF21 and PRDM1 were up-regulated in Karpas-422 cells that contain both wild type and Y641N mutant EZH2 proteins in a dose-dependent manner (Fig. 3S, supplementary material). Conversely, minimal modulation of target gene expression was observed in the wild type EZH2-containing OCI-LY19 cell line, indicating that gene repression was mediated by elevated H3K27Me3 levels in the EZH2-mutant cell line. These results correlated well with the cellular phenotypic effects caused by compound **31** and provided robust cellular biomarkers for subsequent *in vivo* studies.

We also profiled compound **31** in various in vitro ADME assessments in preparation for its use *in vivo*. As shown in Table 5, the molecule displayed reasonable solubility, good permeability, and low efflux potential in these *in vitro* assays. On the other hand, compound **31** also displayed high clearance in a microsomal stability assay for both human and mouse species (Table 5). As shown in Fig. 6, at a 300 mg/kg dose, compound **31** displayed free plasma concentrations above the *in vitro* cell IC_{90} values for at least 6 h.[41] However, at both 100 and 30 mg/kg doses, the free plasma concentrations were either at or below the cell IC_{50} values at the 6 h time point. These results suggested that relatively high doses of **31** would be required to maintain appropriate mouse plasma exposures. We therefore profiled the molecule in a mouse tumor growth inhibition (TGI) experiment to confirm that the novel inhibitor series could demonstrate *in vivo* efficacy.

Accordingly, an *in vivo* efficacy experiment with compound **31** was then designed with dose groups of 200 and 300 mg/kg, twice a day (BID) for 20 days (Figure 7A). Treatment with compound **31** was well tolerated at both doses with less than 10% body weight loss observed

during the course of the experiment (Figure 7B). Tumor volumes were measured every 3-5 days throughout the study. As shown in Figure 7A, on day 20, compound **31** demonstrated tumor stasis or regression at the 200 and 300 mg/kg dose levels, respectively. In addition, tumor growth inhibition was sustained for at least another three weeks after the last dose, demonstrating the ability of compound **31** to mediate long-term epigenetic reprogramming in cells.

On Day 20, the compound dosing was stopped and tumor samples were collected to measure both H3K27Me3 and PRC2 target gene expression levels. Compound **31** induced approximately 55.5% and 66.4% reduction of the H3K27Me3 level at doses of 200 mg/kg and 300 mg/kg, respectively (Figure 7C). In addition, the PRC2 target genes TNFRSF21 and PRDM1 were both strongly upregulated in both the 200 mg/kg and 300 mg/kg dosing arms (Figure 7D). The H3K27Me3 reduction coupled with the strong elevation of the two target genes demonstrated the expected on-target effect for this novel class of EZH2 inhibitors. Importantly, eventual tumor regrowth was strongly correlated with global increases in H3K27Me3 levels and the re-silencing of PRC2 target genes, further solidifying the relationship between the cellular biomarkers and the anti-proliferative effect in this model (Figure 4S, A, B, and C in supplementary material). The observed efficacy and safety profile associated with this tool compound demonstrated proof of concept for this novel class of EZH2 inhibitor as a therapeutic agent in DLBCL harboring EZH2 activating mutations.

CHEMISTRY

Benzoic acids **33a-i** (Scheme 1) were either purchased or synthesized in two steps from commercially available methyl-3-hydroxy benzoates through phenol alkylation followed by ester hydrolysis (see Table 1 for R^1 and R^2). Commercially available 3-(aminomethyl)-4,6-dimethylpyridin-2(1H)-one (**35a)** was then coupled to the benzoic acids under standard amide

coupling conditions (HATU, NMM, DMF) to give **6** and **8-15** as shown in Scheme 1. Compound **7** was made in a similar fashion starting from commercially available 2-methylbenzoic acid.

Scheme 1. Synthesis of benzamides 6 and 8–15

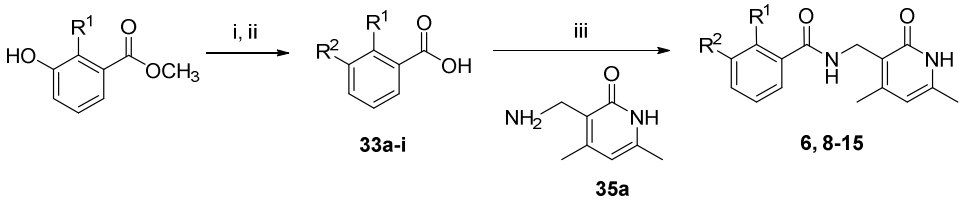

Reagents and conditions: i. Cs_2CO_3, DMF, alkyl bromides or iodides; ii. LiOH, MeOH, 80 °C; iii. HATU, NMM, DMF.

The benzyloxy protected chloromethyl pyridine intermediate **35b** (Scheme **2**) served as a protected dimethylpyridone and allowed for late stage alkylation of various lactams. The commercially available 3-cyano-4,6-dimethylpyridone was protected as the benzyl ether to afford 2-(benzyloxy)-4,6-dimethylnicotinonitrile (**34a**). Iterative reductions then transformed the nitrile to the corresponding aldehyde (**34b**) and then to the primary alcohol (not shown). The latter entity was subsequently converted to the chloromethyl pyridine **35b** using standard chemistries.

Scheme 2: Synthesis of 35b

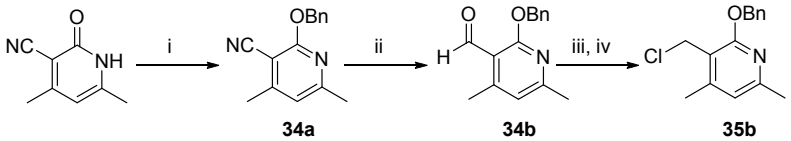

Reagents and conditions: i. BnCl, Ag_2O, toluene, 100 °C; ii. DIBAL, DCM, 0 - 5 °C; iii. $NaBH_4$, MeOH, 25 °C; iv. $SOCl_2$, -40 °C, DCM.

Synthesis of R^1 methyl-substituted dihydroisoquinolin-1(2H)-one **21** (Scheme **3**) was accomplished starting from methyl 6-bromo-3-isopropoxy-2-methylbenzoate[42]. Suzuki coupling with 2-Boc-aminoethyl trifluoroborate yielded compound **36**. Treatment of **36** with HCl deprotected the Boc group from the amine moiety and subsequent heating in the presence of DIEA then generated lactam **37**. Alkylation of the lactam nitrogen of **37** with **35b** followed by hydrogenolysis provided compound **21**.

Scheme 3: Synthesis of 21

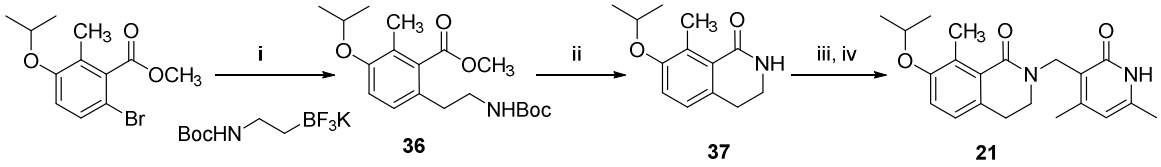

Reagents and conditions: i. Cs_2CO_3, cat. $Pd(OAc)_2$, cat. RuPhos, toluene, H_2O, 95 °C; ii. (a) HCl 1,4-dioxane, 25 °C; (b) DIEA, 80 °C; iii. NaH, THF, **35b**; iv. Pd/C, H_2, MeOH.

Synthesis of various alkoxy-substituted dihydroisoquinolin-1(2H)-ones **18**–**20** and **23** (Scheme 4) was accomplished using a common intermediate **38** that was prepared by regio-selective chlorination of commercially available 7-methoxy-3,4-dihydroisoquinolin-1(2H)-one. The methyl ether present in **38** was cleaved using BBr_3 in DCM to provide **39**. Alkylation of **39** using various electrophiles (such as iodoethane, 2-iodopropane, and (*S*)-tetrahydrofuran-3-yl methanesulfonate) under mildly basic condition provided **40a**-**40c** (see Table 2 for R^3). Subsequent alkylation of the lactam nitrogens present in **38** and **40a**-**40c** with **35b** and de-protection of the benzyl ether using TFA afforded pyridone containing lactams **18**-**20** and **23**.

Scheme 4. Synthesis of 18–20 and 23

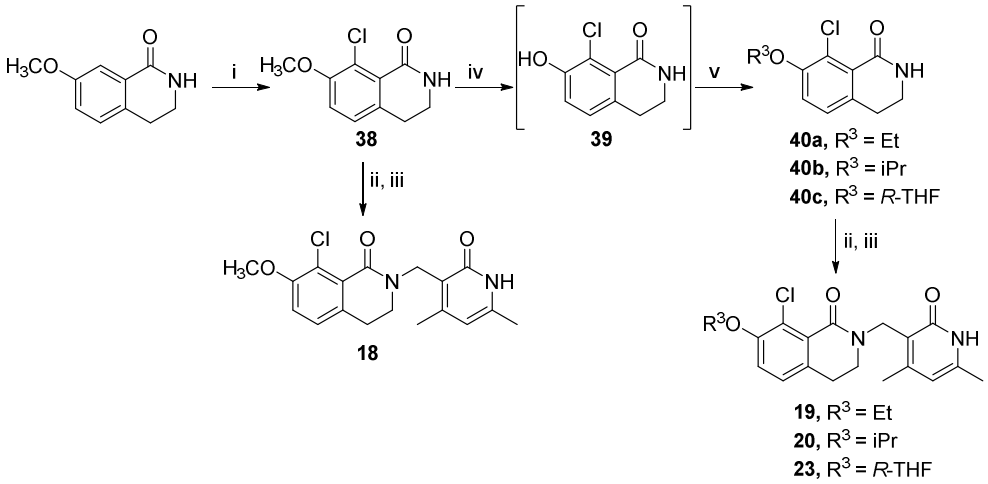

Reagents and conditions: i. NCS, H_2SO_4, 0-25 °C; ii. NaH, DMF, **35b**; iii. TFA, DCM, 25 °C; iv. BBr_3, DCM, 5-25 °C; v. R^3X, DMF, K_2CO_3.

Synthesis of **24**–**26** (Scheme 5) began by using Sandmeyer chemistry to transform the amino group present in **41**[42] to various halogens (F, Cl, I) to provide **42a-c**. The isopropoxy groups of **42a-c** were then removed by treatment with BBr_3 in DCM to afford the corresponding phenols (not shown). These entities were alkylated with (*S*)-tetrahydrofuran-3-yl methanesulfonate[43] to afford the 3-(*R*)-THF intermediates (**43a-c**) *via* SN2 inversion. In the case of compound **25**, the lactam present in **43c** was condensed with **35b** to give the corresponding alkylated lactam (**44**). The iodo group of **44** was subsequently converted to a methyl group via a Suzuki coupling reaction and the resulting product (not shown) was deprotected with TFA in DCM to give **25**. Lactam alkylation of the 3-(*R*)-THF intermediates (**43a** and **43b**) with **35b** followed by benzyl ether deprotection afforded compounds **24** and **26** in modest overall yields.

Scheme 5: Synthesis of 24-26

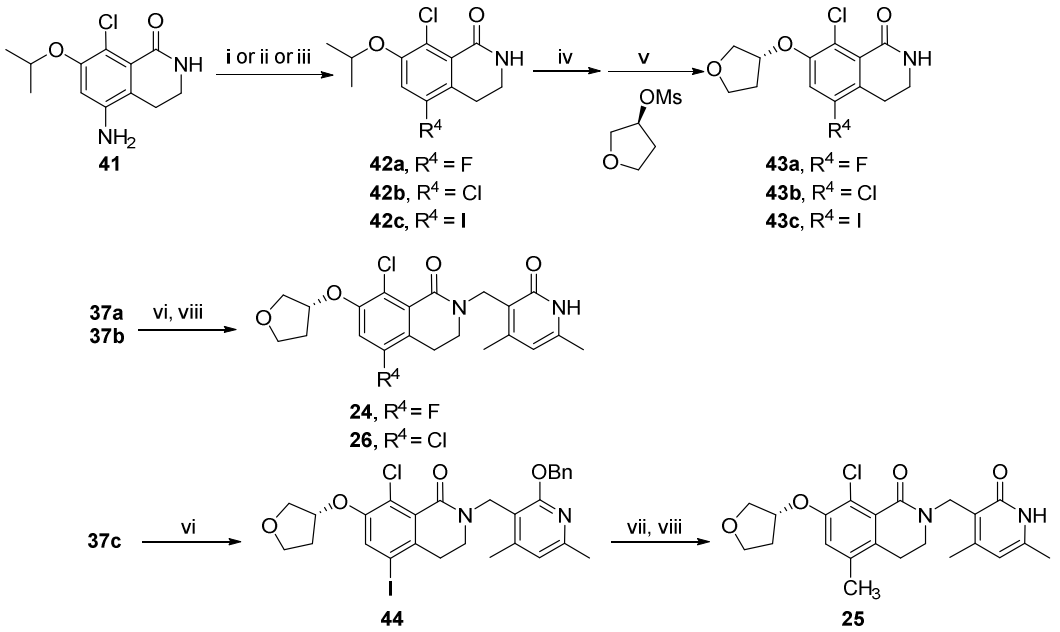

Reagents and conditions: i. HBF_4, $NaNO_2$, H_2O, 0 °C; ii. isoamyl nitrite, CH_3CN, CH_2I_2, 80 °C; iii. $CuCl_2$, LiCl, CH_3CN, isoamyl nitrite, 55 °C; iv. BBr_3, DCM, 5-25 °C; v., DMF, K_2CO_3; vi. NaH, DMF, **35b**; vii. $CH_3B(OH)_2$, Cs_2CO_3, $Pd(dppf)Cl_2$, DME, H_2O, 90 °C; viii. TFA, DCM, 25 °C.

Synthesis of R^2 heteroaryl-containing dihydroisoquinolin-1(2H)-ones **27**–**31** (Scheme 6) started with nitrile reduction ($NiCl_2/NaBH_4$) of 2-(2,5-dichlorophenyl)acetonitrile with concomitant methyl carbamate protection to afford **45** in 54% yield.[44] Intramolecular Friedel-Crafts acylation[45] (TfOH, 80 °C) afforded **46** in 72% yield without chromatography. Bromination of **46** with NBS in concentrated H_2SO_4 cleanly afforded the 7-bromo intermediate (not shown) in 98% yield. Subsequent lactam nitrogen alkylation (**35b**, KOt-Bu, DMF, 0 °C) gave **47** in 85% yield. Introduction of heteroaromatic rings at the 7-position was accomplished using Suzuki cross-coupling reactions with various boronic esters followed by benzyl ether deprotection to afford compounds **27**, **29**, and **31**. In the case of compound **28**, a THP-protected

pyrazole bromide was used in a Suzuki coupling reaction to prepare **48**. Subsequent simultaneous deprotection of both the THP and benzyl ether groups present in **48** then afforded **28**. In the case of compound **30**, the pyrazole present in **29** was selectively alkylated under mildly basic conditions to give the target molecule.

Scheme 6: Synthesis of 27-31

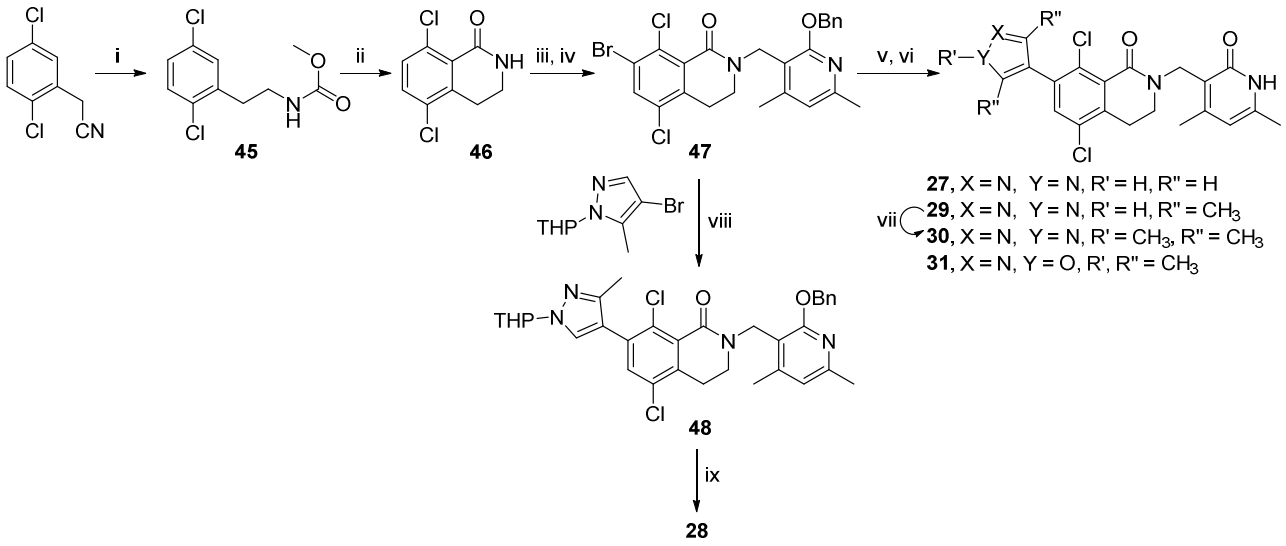

Reagents and conditions: i. $NiCl_2 \bullet 6H_2O$, $NaBH_4$, MeOH, $ClCO_2Me$, 0 °C; ii. TfOH, 0-80 °C; iii. NBS, H_2SO_4; iv. **35b**, KOt-Bu, DMF, 0 °C; v. boronic esters, Pd catalysts, bases; vi. TFA, 25 °C; vii. CH_3I, Cs_2CO_3, DMF, 25 °C; viii. (a) Bis(pinacolato)diboron, $Pd(dppf)Cl_2$, KOAc, dioxane, 95 °C; (b) $Pd(dppf)Cl_2$, Na_2CO_3, dioxane, 95 °C; ix. HCl, EtOH, 70 ^oC.

Synthesis of compound **32** (Scheme 7) started with commercially available 7-amino-3,4-dihydroisoquinolin-1(2H)-one which underwent electrophilic aromatic chlorination with NCS to provide **49**. The amino group present in **49** was transformed to the corresponding bromide using Sandmeyer chemistry and the resulting intermediate (not shown) was alkylated on the lactam nitrogen with compound **35b** to give **50**. Suzuki coupling of **50** with the 3,5-dimethyloxazole boronic ester and subsequent deprotection yielded compound **32**.

Scheme 7: Synthesis of 32

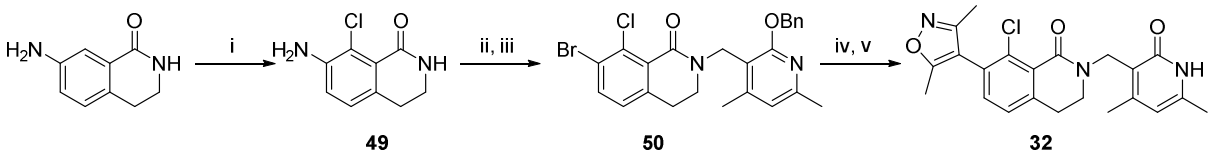

Reagents and conditions: i. NCS, DMF, 55 °C; ii. CuBr, CH_3CN, isoamyl nitrite, 60 °C; iii. KOt-Bu, DMF, **35b**; iv. $Pd(PPh_3)_4$, CsF, 3,5-dimethyl-4-(4,4,5,5-tetramethyl-1,3,2-dioxaborolan-2-yl)isoxazole, dioxane, 110 °C; v. TFA, 25 °C.

Synthesis of the 7-membered ring compound **16** (Scheme **8**) was accomplished via chlorination of the commercially available 8-methoxy-2,3,4,5-tetrahydro-1H-2-benzazepin-1-one to give a mixture of regio-isomers **51a** and **51b** in a ratio of 5.3 to 1 (ratio was assessed based on the individually isolated final products). This mixture was alkylated with compound **35b** and the resulting products (not shown) were subjected to acidic de-protection conditions. Compound **16** was isolated from the resulting mixture *via* preparative HPLC.

The synthesis of compound **17** (Scheme **8**) started with the previously described **34b** (Scheme **2**). Reductive amination of **34b** with ethanolamine yielded compound **52**. Amide coupling of **52** with 2-chloro-6-fluoro-3-methoxy-benzoic acid followed by aromatic substitution resulted in the 7-membered ring intermediate **53**. Subsequent acidic deprotection of the benzyl group provided compound **17**.

Scheme 8: Synthesis of 7-Membered Ring Analogs 16 and 17

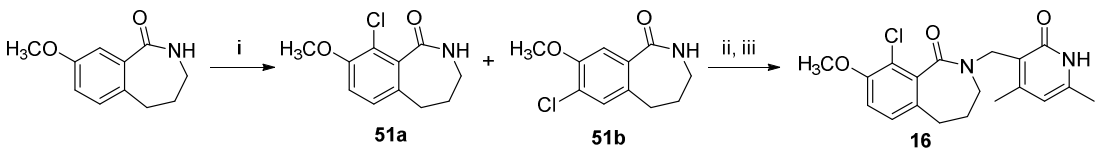

Reagents and conditions: i. NCS, HOAc, 100 °C; ii. NaH, DMF, **35b**, 80 °C; iii. HCl, MeOH, 70 °C.

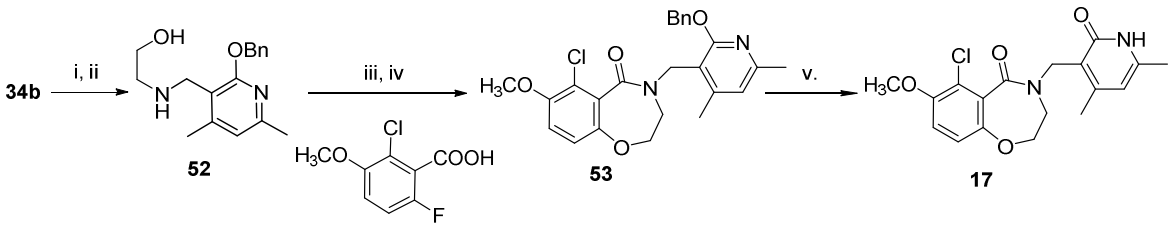

Reagents and conditions: i. DIBAL, DCM, 0-5 °C; ii. $HOCH_2CH_2NH_2$, $NaBH_3CN$, MeOH; iii. HATU, Et_3N, DMF; iv. KOt-Bu, THF/DMF, 100 °C; v. TFA, 60 °C.

CONCLUSION

In summary, a novel series of lactam-containing EZH2 inhibitors was created from an initial benzamide lead (compound **6**) using computational torsional angle analysis coupled with a ligand-cyclization strategy. The ligand lipophilicity efficiency (LipE) and potency of the initial lead were improved considerably during the course of these optimization activities. The 1-2 unit LipE improvement was achieved via lead transformation of benzamides to lactams and by the incorporation of the alkoxy and heteroaryl substituents at the R^2 position (Figure 5). These efforts culminated with the identification of an optimized molecule, compound **31**, which displayed good efficacy in a diffuse large B-cell lymphoma Karpas-422 tumor model and exhibited on-target pharmacodynamic effects in vivo. Further optimization of the pharmaceutical properties of this class of compounds will be reported in due course.

EXPERIMENTAL METHODS

Chemistry

Unless otherwise noted, materials were obtained from commercial suppliers and were used without further purification. Removal of solvent under reduced pressure or concentration refers to distillation using Büchi rotary evaporator attached to a vacuum pump (3 mm Hg). Products

obtained as solids or high boiling oils were dried under vacuum (1 mm Hg). Silica gel chromatography was performed either by CombiFlash (Teledyne ISCO), SP4 or Isolera (Biotage) purification systems. All reactions were performed under a positive pressure of nitrogen, argon, or with a drying tube, at ambient temperature (unless otherwise stated), in anhydrous solvents, unless otherwise indicated. Analytical thin-layer chromatography was performed on glass-backed Silica Gel 60_F 254 plates (Analtech, 0.25mm) and eluted with the appropriate solvent ratios (v/v). The reactions were assayed by high performance liquid chromatography-mass spectrometry (LC-MS) or thin-layer chromatography (TLC) and terminated as judged by the consumption of starting material. LCMS utilized 254 and 220 nm wavelengths and either electrospray ionization (ESI) positive mode or atmospheric-pressure chemical ionization (APCI) in positive mode. The TLC plates were visualized by UV, p-anisaldehyde, phosphomolybdic acid, or iodine staining. Microwave assisted reactions were run in a Biotage Initiator. ^{1}H NMR spectra were recorded on a Bruker XWIN-NMR (400 MHz) spectrometer. Proton resonances are reported in parts per million (ppm) downfield from tetramethylsilane (TMS). ^{1}H NMR data are reported as multiplicity (s, singlet; d, doublet; t, triplet; q, quartet; dd, doublet of doublets; dt, doublet of triplets; brs., broad singlet). For spectra obtained in $CDCl_3$, DMSO-d_6, and CD_3OD, the residual protons (7.27, 2.50, and 3.31 ppm, respectively) were used as the internal reference. The purity of final products was generally >95% as determined by HPLC methods and/or ^{1}H NMR.

General procedure for the synthesis of compounds 6-15:

O-(7-azabenzotriazol-1-yl)-N,N,N′,N′-tetramethyluronium hexafluorophosphate (HATU, 0.515 mmol) and N-methylmorpholine (NMM, 0.515 mmol) were added to a solution of **33a-i** (0.515 mmol) in DMF. The solution was stirred at room temperature for 1 h, then **35a** (0.515 mmol)

and NMM (1.03 mmol) were added. The reaction was stirred at room temp for 2 h and diluted with water. The resulting precipitate was collected by filtration, washed with water, transferred to a vial with methanol/water, frozen and lyophilized to provide compounds **6-15**.

***N*-((4,6-Dimethyl-2-oxo-1,2-dihydropyridin-3-yl)methyl)-3-methoxy-2-methylbenzamide (6)**. **6** was isolated as a white solid. LCMS *m/z* 301 $[M + H]^+$; ^{1}H NMR (400 MHz, $CDCl_3$) δ ppm 10.81 (s, 1H), 7.06 (d, *J* = 8 Hz, 1H), 7.03-6.99 (m, 1H), 6.85 (d, *J* = 7.2 Hz, 1H), 6.77 (d, *J* = 8.4 Hz, 1H), 5.85 (s, 1 H), 4.45 (d, *J* = 6.0 Hz, 2H), 3.74 (s, 3H), 2.32 (s, 3H), 2.16 (s, 3H), 2.13 (s, 3H).

***N*-((4,6-Dimethyl-2-oxo-1,2-dihydropyridin-3-yl)methyl)-2-methylbenzamide (7)**. **7** was isolated as a white solid. LCMS *m/z* 271 $[M + 1]^+$; ^{1}H NMR (400 MHz, DMSO-d_6) δ ppm 11.38 (brs., 1H), 8.08 (t, *J* = 4.2 Hz, 1H), 7.22 - 7.31 (m, 2H), 7.13 - 7.22 (m, 2H), 5.85 (s, 1H), 4.27 (d, *J* = 5.0 Hz, 2H), 2.29 (s, 3H), 2.19 (s, 3H), 2.11 (s, 3 H).

***N*-((4,6-Dimethyl-2-oxo-1,2-dihydropyridin-3-yl)methyl)-3-methoxybenzamide (8)**. **8** was isolated as a white solid. LCMS *m/z* 287 $[M + H]^+$; ^{1}H NMR (400 MHz, DMSO-d_6) δ ppm 11.49 (s, 1H), 8.37 (s, 1H), 7.42-7.30 (m, 3H), 7.06-7.04 (m, 1H), 5.87 (s, 1H), 4.30-4.29 (m, 2H), 3.78 (s, 3H), 2.17 (s, 3H), 2.11 (s, 3H).

***N*-((4,6-Dimethyl-2-oxo-1,2-dihydropyridin-3-yl)methyl)-3-ethoxy-2-methylbenzamide (9)**. **9** was isolated as a white solid. LCMS *m/z* 315 $[M + H]^+$; ^{1}H NMR (400 MHz, $CDCl_3$) δ ppm 11.68 (s, 1H), 7.04-7.00 (m, 2H), 6.83 (d, *J* = 7.6 Hz, 1H), 6.75 (d, *J* = 8.4 Hz, 1H), 5.86 (s, 1H), 4.45 (d, *J* = 6 Hz, 2H), 3.96-3.91 (m, 2H), 2.32 (s, 3H), 2.17 (s, 3H), 2.12 (s, 3H), 1.34 (t, *J* = 6.8 Hz, 3H).

***N*-((4,6-Dimethyl-2-oxo-1,2-dihydropyridin-3-yl)methyl)-3-isopropoxy-2-methylbenzamide (10). 10** was isolated as a white solid. LCMS *m/z* 329 $[M + H]^+$; ^{1}H NMR (400 MHz, CD_3OD)

δ ppm 7.10 - 7.29 (m, 1H), 7.00 (d, *J* = 8.1 Hz, 1H), 6.88 (d, *J* = 7.6 Hz, 1H), 6.13 (s, 1H), 4.61 (dt, *J* = 12 Hz, 6.1 Hz, 1H), 4.49 (s, 2H), 2.41 (s, 3H), 2.27 (s, 3H), 2.19 (s, 3H), 1.34 (d, *J* = 6.1 Hz, 6H).

***N*-((4,6-Dimethyl-2-oxo-1,2-dihydropyridin-3-yl)methyl)-2-fluoro-3-methoxybenzamide (11)**. **11** was isolated as a white solid. LCMS *m/z* 305 $[M + H]^+$; ^{1}H NMR (400 MHz, $CDCl_3$) δ ppm 11.5 (s, 1H), 8.26 (s, 1H), 7.24-7.12(m, 3H), 5.87 (s, 1H), 4.28 (d, *J* = 4.8 Hz, 2H), 3.84(s, 3H), 2.18 (s, 3H), 2.11 (s, 3H).

***N*-((4,6-Dimethyl-2-oxo-1,2-dihydropyridin-3-yl)methyl)-2,3-dimethoxybenzamide (12)**. **12** was isolated as a white solid. LCMS *m/z* 339 $[M + H + Na]^+$; ^{1}H NMR (400 MHz, DMSO-d_6) δ ppm 11.6 (brs., 1H), 8.68 (t, *J* = 5.6 Hz, 1H), 7.34 (dd, *J* = 7.6, 2.0 Hz, 1H), 7.18 (d, *J* = 6.4 Hz, 1H), 7.13 (t, 8.0 Hz, 1H), 5.88 (s, 1H), 4.31 (d, *J* = 6.0 Hz, 1H), 3.83 (s, 2H), 3.75 (s, 3H), 2.24 (s, 3H), 2.11 (s, 3H).

***N*-((4,6-Dimethyl-2-oxo-1,2-dihydropyridin-3-yl)methyl)-2-hydroxy-3-methoxybenzamide (13)**. **13** was isolated as a white solid. LCMS *m/z* 324 $[M + H + Na]^+$; ^{1}H NMR (400 MHz, DMSO-d_6) δ ppm 12.3 (brs., 1H), 11.6 (brs., 1H), 8.78 (t, *J* = 5.6 Hz, 1H), 7.46 (dd, *J* = 7.6, 2.0 Hz, 1H), 7.08 (d, *J* = 6.4 Hz, 1H), 6.77 (t, *J* = 8.0 Hz, 1H), 5.88 (s, 1H), 4.32 (d, *J* = 6.0 Hz, 1H), 3.78 (s, 2H), 3.35 (s, 3H), 2.19 (s, 3H), 2.12 (s, 3H).

2-Chloro-N-((4,6-dimethyl-2-oxo-1,2-dihydropyridin-3-yl)methyl)-3-methoxybenzamide (14). **14** was isolated as a white solid. LCMS m/z 321 $[M + H]^+$; (400 MHz, DMSO-d_6) δ ppm 11.45 (brs., 1H), 8.25 (t, *J* = 4.8 Hz, 1H), 7.23-7.34 (m, 1H), 7.14 (d, *J* = 8.1 Hz, 1H), 6.90 (d, *J* = 7.6 Hz, 1H), 5.86 (s, 1H), 4.27 (d, *J* = 5.1 Hz, 2H), 3.85 (s, 3H), 2.18 (s, 3H), 2.11 (s, 3H).

2-Chloro-N-((4,6-dimethyl-2-oxo-1,2-dihydropyridin-3-yl)methyl)-3-isopropoxybenzamide (15). **15** was isolated as a white solid. LCMS *m/z* 350 $[M + H]^+$; ^{1}H NMR (400 MHz, DMSO-

d_6) δ ppm 11.44 (brs., 1H), 8.23 (t, J = 4.8 Hz, 1H), 7.21-7.30 (m, 1H), 7.11-7.19 (m, 1H), 6.87 (dd, J = 1.4, 7.5 Hz, 1H), 5.85 (s, 1H), 4.65 (td, J = 6.0, 12.1 Hz, 1H), 4.26 (d, J = 5.1 Hz, 2H), 2.18 (s, 3H), 2.10 (s, 3H), 1.28 (d, J = 6.1 Hz, 6H).

9-Chloro-2-((4,6-dimethyl-2-oxo-1,2-dihydropyridin-3-yl)methyl)-8-methoxy-2,3,4,5-tetrahydro-1H-benzo[c]azepin-1-one (16). A solution of commercial 8-methoxy-2,3,4,5-tetrahydro-1H-2-benzazepin-1-one (25.0 mg, 0.154 mmol) and NCS (20.6 mg, 0.154 mmol) in HOAc (3 mL) was stirred at 100 °C for 4.5 h. The reaction mixture was partitioned between EtOAc (20 mL) and water (20 mL). The organic phase was dried over sodium sulfate, and concentrated under vacuum to give a mixture of 9-chloro-8-methoxy-2,3,4,5-tetrahydro-1H-2-benzazepin-1-one (**51a**) and 7-chloro-8-methoxy-2,3,4,5-tetrahydro-1H-2-benzazepin-1-one (**51b)** (35 mg, 100%) as a colorless oil. To this mixture of 7-ring lactams (35.0 mg, 0.150 mmol) in DMF (5 mL) was added **35b** (47 mg, 0.180 mmol) and NaH (9 mg, 0.225 mmol, 60% dispersion in mineral oil). The reaction mixture was heated at 80 °C for 24 h. The reaction mixture was poured into a NaOAc-HOAc buffer (5 mL) and extracted with EtOAc (2 x 10 mL). The combined organic layers were dried over sodium sulfate and concentrated under vacuum. The resulting brown oil was dissolved in MeOH (1 mL) and HCl (0.05 mL of 3 M in n-butanol) was added. The reaction mixture was heated at 70 °C for 24 h. The solvent was removed *in vacuo* and the residue was purified by preparative HPLC to give **16** as the first eluting product (20 mg, 36%). LCMS *m/z* 361 $[M + 1]^+$; ^{1}H NMR (400 MHz, CD_3OD) δ ppm 7.09-7.14 (m, 1H), 7.05-7.10 (m, 1H), 6.13 (s, 1H), 4.89 (s, 1H), 4.71-4.79 (m, 1H), 3.88 (s, 3H), 3.38 (dd, J = 5.9, 14.9 Hz, 1H), 2.92-3.01 (m, 1H), 2.57-2.73 (m, 2H), 2.35 (s, 3H), 2.25 (s, 3H), 2.06-2.14 (m, 1H), 1.53-1.64 (m, 1H).

6-Chloro-4-((4,6-dimethyl-2-oxo-1,2-dihydropyridin-3-yl)methyl)-7-methoxy-3,4-dihydrobenzo[f][1,4]oxazepin-5(2H)-one (17). To a solution of 2-chloro-6-fluoro-3-methoxy-benzoic acid (1.00 g, 4.89 mmol) in anhydrous DMF (30 mL) were added HATU (2.30 g, 5.85 mmol) and Et_3N (1.36 mL, 9.76 mmol). The reaction mixture was stirred for 5 min. and 2-[(2-benzyloxy-4,6-dimethyl-pyridin-3-ylmethyl)-amino]-ethanol (**52**, 1.47 g, 5.12 mmol) was added as a solid in one portion. The resulting reaction mixture was stirred at room temperature for 2 h. The reaction mixture was partitioned between ethyl acetate (200 mL) and water (200 mL). The organic phase was separated, washed with brine (2 x 200 mL), dried over sodium sulfate, and concentrated under vacuum to give N-(2-benzyloxy-4,6-dimethylpyridin-3-ylmethyl)-2-chloro-6-fluoro-N-(2-hydroxyethyl)-3-methoxybenzamide (2.31 g, 100%) as a gum. To a solution of N-(2-benzyloxy-4,6-dimethyl-pyridin-3-ylmethyl)-2-chloro-6-fluoro-N-(2-hydroxy-ethyl)-3-methoxy-benzamide (2.31 g, 4.88 mmol) in anhydrous DMF (20 mL) was added KOt-Bu (12.2 mL of 1 M solution in THF, 12.2 mmol). The reaction mixture was stirred at 100 °C for 3 h. After cooling to room temperature, the reaction mixture was partitioned between EtOAc (200 mL) and water (200 mL). The organic phase was separated, washed with brine (2 x 200 mL), dried over sodium sulfate, and concentrated under vacuum. The residue was purified by column chromatography (heptanes/EtOAc) to give 4-((2-(benzyloxy)-4,6-dimethylpyridin-3-yl)methyl)-6-chloro-7-methoxy-3,4-dihydrobenzo[f][1,4]oxazepin-5(2H)-one (**53**, 668 mg, 30% yield) as a solid. LCMS m/z 453 $[M + H]^+$; ^1H NMR (400 MHz, $CDCl_3$) δ ppm 7.41 - 7.46 (m, 2H), 7.29 - 7.39 (m, 3H), 6.84 - 6.95 (m, 2H), 6.68 (s, 1H), 5.42 (s, 2H), 4.97 (s, 2H), 3.88 (s, 3H), 3.73 (t, *J* = 5.4 Hz, 2H), 3.22 (t, *J* = 5.4 Hz, 2H), 2.44 (s, 3H), 2.39 (s, 3H). A mixture of **53** (636 mg, 1.40 mmol) in TFA (10 mL) was stirred at 60 °C for 3 h. The TFA was removed in vacuum and the resulting residue was partitioned between ether (100 mL) and satd. aq. sodium bicarbonate (100

mL). The organic phase was separated, and washed with brine (100 mL), dried over sodium sulfate, and concentrated under vacuum to give **17** (503 mg, 99%) as a white solid. LCMS *m/z* 363 $[M + 1]^+$; ^{1}H NMR (400 MHz, $CDCl_3$) δ ppm 12.59 (brs., 1H), 6.88 - 6.97 (m, 2H), 6.04 (s, 1H), 4.90 (s, 2H), 4.03 (brs., 2H), 3.89 (s, 3H), 3.54 (t, *J* = 5.4 Hz, 2H), 2.41 (s, 3H), 2.30 (s, 3H).

8-Chloro-2-((4,6-dimethyl-2-oxo-1,2-dihydropyridin-3-yl)methyl)-7-methoxy-3,4-dihydroisoquinolin-1(2H)-one (18). To a solution of compound **38** (80 mg, 0.38 mmol) in dry DMF (2 mL) was added NaH (27 mg, 1.14 mmol, 60% in mineral oil) at 0 °C. The mixture was stirred at 0 °C for 30 min. To the mixture was added compound **35b** (198 mg, 0.76 mmol). The mixture was stirred at room temperature for 14 h. To the mixture was added EtOAc (20 mL). The mixture was washed with brine (4 x 20 mL), dried over Na_2SO_4 and concentrated *in vacuo*. The residue was purified by flash chromatography (petroleum ether/EtOAc= 2/1) to give 2-((2-(benzyloxy)-4,6-dimethylpyridin-3-yl)methyl)-8-chloro-7-methoxy-3,4-dihydroisoquinolin-1(2H)-one (90 mg, 54%) as a yellow oil. Benzyl deprotection was conducted by dissolving the intermediate (60 mg, 0.14 mmol) in DCM (3 mL) and adding TFA (3 mL). After stirring the mixture at room temperature for 3 h, the reaction was concentrated *in vacuo* and the residue was purified by flash chromatography (DCM/MeOH = 10:1, R_f = 0.4) to give **18** (26 mg, 54%) as a white solid. LCMS m/z 347 $[M + H]^+$; ^{1}H NMR (400 MHz, $CDCl_3$) δ ppm 7.14 (s, 2H), 6.11 (s, 1H), 4.77 (s, 2H), 3.88 (s, 3H), 3.45 (t, *J* = 6.2 Hz, 2H), 3.21 (t, *J* = 6.2 Hz, 2H), 2.28 (s, 3H), 2.24 (s, 3H).

8-Chloro-2-((4,6-dimethyl-2-oxo-1,2-dihydropyridin-3-yl)methyl)-7-ethoxy-3,4-dihydroisoquinolin-1(2H)-one (19). To a solution of **38** (0.50 g, 2.4 mmol) in dry DCM (20 mL) was added BBr_3 (0.6 mL, 5.9 mmol) at 5 °C. The mixture was stirred at room temperature

for 14 h. To the reaction mixture was added dropwise H_2O (20 mL). The mixture was extracted with EtOAc (2 x 30 mL). The combined organic layers were washed with brine (40 mL), dried over Na_2SO_4 and concentrated *in vacuo* to give 8-chloro-7-hydroxy-3,4-dihydroisoquinolin-1(2H)-one (**39**, 0.5 g, 100%) as a brown solid. This intermediate was taken to the next step without further purification. To a mixture of crude **39** (0.47 g, 2.4 mmol) and K_2CO_3 (0.99 g, 7.2 mmol) in dry DMF (10 mL) was added dropwise iodoethane (0.37 g, 2.9 mmol) at room temperature. The mixture was stirred at room temperature for 14 h. The reaction mixture was partitioned between brine (50 mL) and EtOAc (40 mL). The aqueous layer was extracted with EtOAc (4 x 40 mL). The combined organic layers were dried (Na_2SO_4) and concentrated *in vacuo*. The residue was purified by flash chromatography (petroleum ether/EtOAc = 1/1, R_f ~ 0.3) to give 8-chloro-7-ethoxy-3,4-dihydroisoquinolin-1(2H)-one (**40a,** 0.35 g, 64%) as a brown solid. By an analogous procedure used to make **18** from **38**, **19** was obtained as a white solid from **40a**. LCMS m/z 361 $[M+H]^+$; ^{1}H NMR (400 MHz, $CDCl_3$) δ ppm 11.03 (s, 1H), 6.98-6.91 (m, 2H), 5.93 (s, 1H), 4.79 (s, 2H), 4.11-4.05 (m, 2H), 3.56 (t, *J* = 6.2 Hz, 2H), 2.76 (t, *J* = 6.2 Hz, 2H), 2.34 (s, 3H), 2.25 (s, 3H), 1.45 (t, *J* = 6.2 Hz, 3H).

8-Chloro-2-((4,6-dimethyl-2-oxo-1,2-dihydropyridin-3-yl)methyl)-7-isopropoxy-3,4-dihydroisoquinolin-1(2H)-one (20). **20** was prepared from **40b** using an analogous procedure described for the synthesis of **19** but substituting iodoethane with 2-iodopropane. **20** was isolated as a white solid. LCMS m/z 375 $[M+1]^+$; ^{1}H NMR (400 MHz, DMSO-d_6) δ ppm 11.53 (brs., 1 H), 7.21 (d, *J* = 8.3 Hz, 1H), 7.14 (d, *J* = 8.4 Hz, 1H), 5.88 (s, 1H), 4.58-4.66 (m, 1H), 4.56 (s, 2H), 3.35-3.40 (m, 2H), 2.73 (t, *J* = 6.1 Hz, 2H), 2.15 (s, 3H), 2.12 (s, 3H), 1.27 (d, *J* = 6.1 Hz, 6H).

2-[(4,6-Dimethyl-2-oxo-1,2-dihydropyridin-3-yl)methyl]-8-methyl-7-(propan-2-yloxy)-3,4-dihydroisoquinolin-1(2H)-one (21). A mixture of methyl 6-bromo-2-methyl-3-(propan-2-yloxy)benzoate[41] (154 mg, 0.536 mmol), potassium {2-[(tert-butoxycarbonyl)amino]ethyl}(trifluoro)borate (269 mg, 1.07 mmol) and Cs_2CO_3 (613 mg, 1.88 mmol) in a 3:1 mixture of toluene:water (2.2 mL) was degassed with N_2. Palladium acetate ($Pd(OAc)_2$, 7.2 mg, 0.032 mmol) and RuPhos (30 mg, 0.064 mmol) were added and the mixture was degassed with N_2 and heated at 95 °C for 19 h. The reaction mixture was cooled to room temperature then acidified with 10% aqueous HCl to pH 6 and extracted with EtOAc (20 mL). The organic layer was washed with brine (5 mL), dried over Na_2SO_4, filtered, and concentrated under vacuum. After purification by flash chromatography (EtOAc/heptanes, 0-100%) methyl 6-(2-((tert-butoxycarbonyl)amino)ethyl)-3-isopropoxy-2-methylbenzoate (**36)** was obtained. **36** was then dissolved in DCM (2 mL) and 4N HCl in 1,4-dioxane (0.3 mL) was added. After 16 h, the reaction was concentrated to an oil under vacuum. The residue was dissolved in 1,4-dioxane (3 mL) and DIEA (0.025 mL) was added. The mixture was heated at 80 °C for 50 h, concentrated under vacuum, and purified by column chromatography (EtOAc /heptanes, 0-100) to give 8-methyl-7-(propan-2-yloxy)-3,4-dihydroisoquinolin-1(2H)-one (**37**, 19 mg, 16%) as a white solid. To a 0 °C solution of **37** (30 mg, 0.14 mmol) in THF (0.46 mL) was added 60% sodium hydride (18 mg, 0.45 mmol). After 30 min., 2-(benzyloxy)-3-(chloromethyl)-4,6-dimethylpyridine, **35b** (43 mg, 0.16 mmol) was added and the resulting mixture was heated at 50 °C for 16 h. The reaction mixture was quenched with water (1 mL) and extracted with EtOAc (20 mL), washed with brine (2 mL), dried over sodium sulfate, filtered, and concentrated under vacuum. The residue was purified by column chromatography (EtOAc/heptanes, 0-100), to give 2-{[2-(benzyloxy)-4,6-dimethylpyridin-3-yl]methyl}-8-methyl-7-(propan-2-yloxy)-3,4-

dihydroisoquinolin-1(2H)-one (46 mg, 76%) as a colorless oil which was deprotected using 10% palladium on carbon (10 mg) in MeOH (3 mL) under 1 atmosphere of H_2 for 26 hours. The reaction mixture was filtered through CELITE® and the filtrate was concentrated under vacuum. The residue was purified by column chromatography (EtOAc/heptanes, 50/50-100/0 then EtOAc/MeOH, 100/0 - 70/30), to give **21** (27 mg, 74% yield) as a white solid. LCMS *m/z* 355 (M + H); ^{1}H NMR (400 MHz, $CDCl_3$) δ ppm 12.47 (brs., 1H), 6.89 (s, 2H), 5.93 (s, 1H), 4.84 (s, 2H), 4.43 (td, *J* = 6.1, 11.9 Hz, 1H), 3.49 (t, *J* = 6.1 Hz, 2H), 2.74 (t, *J* = 6.1 Hz, 2H), 2.58 (s, 3H), 2.30 (s, 3H), 2.28 (s, 3H), 1.33 (d, *J* = 6.1 Hz, 6H).

2-((4,6-Dimethyl-2-oxo-1,2-dihydropyridin-3-yl)methyl)-7-isopropoxy-3,4-dihydroisoquinolin-1(2H)-one (22)

2-Iodopropane (0.24 g, 1.44 mmol) was added to a solution of commercially available 7-hydroxy-3,4-dihydroisoquinolin-1(2H)-one (0.2 g, 1.2 mmol) and K_2CO_3 (0.33 g, 2.4 mmol) in acetone (10 mL). The mixture was stirred at 50 °C for 12h. TLC (100% EtOAc) showed the reaction was complete. The mixture was filtered and the filtrate was concentrated *in vacuo* to give the crude product, which was purified by Biotage (Petroleum ether/EtOAc = 1:1, R_f = 0.2) to obtain 7-isopropoxy-3,4-dihydroisoquinolin-1(2H)-one (0.19 g, 77%) as a white solid. To a stirred solution of 7-isopropoxy-3,4-dihydroisoquinolin-1(2H)-one (0.19 g, 0.93 mmol) in THF (5 mL) was added NaH (0.045 g, 0.63 mmol, 60% in oil) at 0 °C under N2. After stirring at 0 °C for 30 min, **35b** (0.24 g, 0.93 mmol) was added and stirred at 50 °C overnight. TLC (petroleum ether/EtOAc = 6:1) showed the reaction was complete. The mixture was concentrated *in vacuo* to give the crude product, which was purified by Biotage (Petroleum ether/EtOAc = 6:1, R_f = 0.5) to obtain compound **22** (0.15 g, 50%) as a white solid. LCMS m/z 341 $[M + H]^+$; LCMS m/z 341 $[M + H]^+$; ^{1}H NMR (400 MHz, CD_3OD) δ ppm 7.49 (d, *J* = 2.8

Hz, 1H), 7.14 (d, *J* = 8.4 Hz, 1H), 7.00 (dd, *J* = 2.8, 8.4 Hz, 1H), 6.12 (s, 1H), 4.76 (s, 2H), 4.66-4.60 (m, 1H), 3.56-3.52 (m, 2H), 2.85-2.82 (m, 2H), 2.30 (s, 3H), 2.26 (s, 3H), 1.33 (d, *J* = 6 Hz, 6H).

(*R*)-8-Chloro-2-((4,6-dimethyl-2-oxo-1,2-dihydropyridin-3-yl)methyl)-7-((tetrahydrofuran-3-yl)oxy)-3,4-dihydroisoquinolin-1(2H)-one (23). **23** was prepared from **40c** using a procedure analogous to that described for the synthesis of **19** but substituting (*S*)-tetrahydrofuran-3-yl methanesulfonate in place of iodoethane. LCMS *m/z* 403 $[M+1]^+$; ^{1}H NMR (400 MHz, DMSO-d_6) δ ppm 11.30 (brs., 1H), 7.20 (d, *J* = 8.3 Hz, 1H), 7.16 (d, *J* = 8.3 Hz, 1H), 5.87 (s, 1H), 5.05-5.10 (m, 1H), 4.57 (s, 2H), 3.73 - 3.92 (m, 4H), 3.37 (t, *J* = 6.1 Hz, 2H), 2.74 (t, *J* = 6.1 Hz, 2H), 2.16 - 2.25 (m, 1H), 2.14 (s, 3H), 2.11 (s, 3H), 1.92-2.01 (m, 1H).

(*R*)-8-Chloro-2-((4,6-dimethyl-2-oxo-1,2-dihydropyridin-3-yl)methyl)-5-fluoro-7-((tetrahydrofuran-3-yl)oxy)-3,4-dihydroisoquinolin-1(2H)-one (24). **24** was prepared from **42a** using a procedure analogous to that described for the synthesis of **19** but substituting (*S*)-tetrahydrofuran-3-yl methanesulfonate in place of iodoethane. LCMS *m/z* 421 $[M+H]^+$; ^{1}H NMR (400 MHz, $CDCl_3$) δ ppm 12.7-12.5 (brs., 1H), 6.72-6.70 (d, *J* = 9.6 Hz, 1H), 6.15 (s, 1H), 4.89 (m, 1H), 4.73 (s, 2H), 4.02-3.94 (m, 4H), 3.65-3.50 (m, 2H), 2.80-2.77 (m, 2H), 2.19 (s, 3H), 2.17 (s, 3H), 2.16-2.15 (m, 2H).

(*R*)-8-Chloro-2-((4,6-dimethyl-2-oxo-1,2-dihydropyridin-3-yl)methyl)-5-methyl-7-((tetrahydrofuran-3-yl)oxy)-3,4-dihydroisoquinolin-1(2H)-one (25). A glass reaction tube was charged with a mixture of **44** (140 mg, 0.226 mmol), methylboronic acid (27 mg, 0.45 mmol) and Cs_2CO_3 (148 mg, 0.453 mmol) in DME (6 mL) and H_2O (1.2 mL) was added Pd(dppf)Cl_2 (11 mg, 0.014 mmol). The mixture was bubbled with N_2 for 1 min., sealed and heated at 90 °C for 16 h. The mixture was diluted with EtOAc (20 mL) and washed with H_2O

(20 mL), brine (20 mL), dried over Na_2SO_4 and concentrated. The residue was purified by flash chromatography (petroleum ether/EtOAc = 1:1) to give the product (100 mg, 68%) as colorless syrup. This syrup (100 mg, 0.197 mmol) was dissolved in DCM (2.5 mL) and TFA (2.5 mL) was added. The mixture was stirred at 25 °C for 16 h. The mixture was concentrated and purified by prep. HPLC [Column: DIKMA Diamonsil (2) C18 200*20 mm*5 um mobile phase from 25%-45% MeCN in water with 0.225% formic acid.] The fractions containing the product were frozen and lyophilized to give **25** (42 mg, 51%) as a white solid. LCMS: *m/z* 417 $[M+1]^+$; ^1H NMR (400 MHz, $CDCl_3$) δ ppm 12.20 (brs., 1H), 6.79 (s, 1H), 6.02 (s, 1H), 4.93 (m, 1H), 4.78 (s, 2H), 4.04-3.92 (m, 4H), 3.56 (m, 2H), 2.69 (m, 2H), 2.37 (s, 3H), 2.31 (s, 3H), 2.22 (s, 3H), 2.19-2.16 (m, 2H).

(*R*)-5,8-Dichloro-2-((4,6-dimethyl-2-oxo-1,2-dihydropyridin-3-yl)methyl)-7-((tetrahydrofuran-3-yl)oxy)-3,4-dihydroisoquinolin-1(2H)-one (26). **26** was prepared from **43b** using a procedure analogous to that described for the synthesis of **19** but substituting (*S*)-tetrahydrofuran-3-yl methanesulfonate in place of iodoethane. LCMS *m/z* 437 $[M + 1]^+$; ^1H NMR (400 MHz, DMSO-d_6) δ ppm 11.56 (s, 1H), 7.42 (s, 1H), 5.89 (s, 1H), 5.18 (s, 1H), 4.56 (s, 2H), 3.79-3.90 (m, 4H), 3.41-3.43 (m, 2H), 2.80-2.83 (m, 2H), 2.19-2.27 (m, 1H), 2.15 (s, 3H), 2.13 (s, 3H), 1.91-1.99 (m, 1H).

5,8-Dichloro-2-[(4,6-dimethyl-2-oxo-1,2-dihydropyridin-3-yl)methyl]-7-(1H-pyrazol-4-yl)-3,4-dihydroisoquinolin-1(2H)-one (27). To a mixture of **47** (200 mg, 0.38 mmol), 1-Boc-4-(4,4,5,5-tetramethyl-1,3,2-dioxaborolan-2-yl)pyrazole (150 mg, 0.50 mmol) and K_2CO_3 (159 mg, 1.15 mmol) in DME (10 mL) and H_2O (0.77 mL) was added 1,1'-bis(diphenylphosphino)ferrocene palladium dichloride ($Pd(dppf)Cl_2$, 66 mg, 0.077 mmol). The resulting mixture was degassed with N_2 and then heated at 100 °C overnight. The mixture was

diluted with H_2O (30 mL) and then extracted with EtOAc (2 x 50 mL). The combined organic layers dried over Na_2SO_4, filtered, and concentrated. The residue was purified by flash chromatography (hexane/EtOAc = 1:1) to give the N-Boc intermediate (170 mg, 87%) as a brown oil. This intermediate (170 mg, 0.336 mmol) was stirred with HCl (3.0 mL of 3 M in 1-butanol, 9.0 mmol) at 70 °C for 3 h. The mixture was concentrated *in vacuo* and the residue was purified by purified by SFC on a HADP column with 10 mM NH_3 in methanol to give **27** (22 mg, 16%) as a white solid. LCMS m/z 417 $[M + H]^+$; HRMS calcd for $C_{20}H_{18}Cl_2N_4O_2$ $[M+H]^+$ 416.0821, found 416.0807; ^{1}HNMR (400 MHz, DMSO-d_6) δ 13.09 (brs., 1H), 11.48 (brs., 1H), 8.16 (brs., 1 H), 7.89 (brs., 1 H), 7.72 (s, 1 H), 5.90 (s, 1 H), 4.58 (s, 2 H), 3.16 (s, 1 H), 2.88 (t, *J* = 5.2 Hz, 2 H), 2.54 (brs., 1 H), 2.16 (s, 3 H), 2.13 (s, 3 H).

5,8-Dichloro-2-(4,6-dimethyl-2-oxo-1,2-dihydro-pyridin-3-ylmethyl)-7-(3-methyl-1H-pyrazol-4-yl)-3,4-dihydro-2H-isoquinolin-1-one (28). 2-(2-Benzyloxy-4,6-dimethyl-pyridin-3-ylmethyl)-5,8-dichloro-7-[3-methyl-1-(tetrahydro-pyran-2-yl)-1H-pyrazol-4-yl]-3,4-dihydro-2H-isoquinolin-1-one (**48**, 40 mg, 0.07 mmol, 1.0 eq) was dissolved in EtOH (1.0 mL) and HCl (0.25 mL, 3 M in 1-butanol, 0.7 mmol, 10 eq) was added. The clear solution was placed in a sand bath at 70 ^{o}C. After three hours, LCMS of the clear solution gave >95% product and no starting material. The reaction was quenched with 50% saturated $NaHCO_3$ and diluted with EtOAc. The layers were separated and the aqueous layer was extracted with EtOAc. The combined organic layers were washed with brine, dried over $MgSO_4$, filtered and concentrated under reduced pressure. TLC (5% methanol-dichloromethane with 0.1% NH_3) gave R_f 0.4 and R_f 0.0. The crude product was purified over silica gel (2 mm chromatotron plate), which was eluted with 1-7% CH_3OH-DCM with 0.1% NH_3, and gave 11 mg (40% yield) of compound **28** as a white solid from ethyl acetate-heptane. TLC (5% methanol-dichloromethane with 0.1%

NH_3) gave R_f 0.4; LCMS *m/z* 431 $[M+1]^+$; ^1H NMR (400 MHz, DMSO-d_6) δ 12.71 (brs., 1H), 11.54 (brs., 1H), 7.72 (brs., 1H), 7.49 (s, 1H), 5.89 (s, 1H), 4.58 (s, 2H), 3.48 (t, J = 6.0 Hz, 2H), 2.91 (t, J = 6.0 Hz, 2H), 2.13-2.17 (m, 9H).

5,8-Dichloro-7-(3,5-dimethyl-1H-pyrazol-4-yl)-2-((4,6-dimethyl-2-oxo-1,2-dihydropyridin-3-yl)methyl)-3,4-dihydroisoquinolin-1(2H)-one (29). A glass reaction tube was charged with a mixture of 2-((2-(benzyloxy)-4,6-dimethylpyridin-3-yl)methyl)-7-bromo-5,8-dichloro-3,4-dihydroisoquinolin-1(2H)-one (**47**, 500 mg, 0.961 mmol), tert-butyl 3,5-dimethyl-4-(4,4,5,5-tetramethyl-1,3,2-dioxaborolan-2-yl)-1H-pyrazole-1-carboxylate (460 mg, 1.43 mmol), K_3PO_4 (408 mg, 1.92 mmol), toluene (15 mL), and H_2O (1.5 mL). $Pd(OAc)_2$ (32.4 mg, 0.144 mmol) and SPhos (2-Dicyclohexylphosphino-2',6'-dimethoxybiphenyl) (118 mg, 0.288 mmol) were added and the resulting mixture was degassed with N_2. The tube was sealed and then heated at 120 °C overnight with stirring. The mixture was diluted with H_2O (20 mL) and then extracted with EtOAc. The combined organic layers were washed with brine (20 mL), dried over Na_2SO_4 and concentrated. The residue was purified by flash chromatography (petroleum ether/EtOAc = 3:1, R_f~0.3) to give *tert*-butyl 4-(2-((2-(benzyloxy)-4,6-dimethylpyridin-3-yl)methyl)-5,8-dichloro-1-oxo-1,2,3,4-tetrahydroisoquinolin-7-yl)-3,5-dimethyl-1H-pyrazole-1-carboxylate (290 mg, 47%) as a yellow gum which was treated with TFA (8 mL) and DCM (8 mL) at room temperature overnight. The mixture was concentrated *in vacuo* and the residue was treated with satd. aq. $NaHCO_3$ (15 mL). The mixture was extracted with DCM (2 x 20 mL) and the organic layers were washed with brine (20 mL), dried over Na_2SO_4 and concentrated. The residue was purified by flash chromatography (DCM/MeOH = 10:1, R_f ~0.5) to give **29** (135 mg, 64%) as a yellow solid. LCMS m/z 445 $[M + H]^+$; ^1H NMR (400 MHz, $CDCl_3$) δ ppm 7.30 (s, 1H), 5.96 (s,

1H), 4.81 (s, 2H), 3.73 (t, *J* = 6.0 Hz, 2H), 3.00 (t, *J* = 6.4 Hz, 2H), 2.39 (s, 3H), 2.31 (s, 3H), 2.16 (s, 6H).

5,8-Dichloro-2-((4,6-dimethyl-2-oxo-1,2-dihydropyridin-3-yl)methyl)-7-(1,3,5-trimethyl-1H-pyrazol-4-yl)-3,4-dihydroisoquinolin-1(2H)-one (30). To a suspension of 5,8-dichloro-7-(3,5-dimethyl-1H-pyrazol-4-yl)-2-((4,6-dimethyl-2-oxo-1,2-dihydropyridin-3-yl)methyl)-3,4-dihydroisoquinolin-1(2H)-one, **29** (31.0 mg, 0.0696 mmol) in DMF (1.0 mL) was added Cs_2CO_3 (25.0 mg, 0.076 mmol) and iodomethane (11 mg, 0.080 mmol). The reaction was stirred for 2 h at room temperature. DMSO (0.5 mL) was added and the reaction was stirred for 16 h at room temperature. Additional iodomethane (11 mg, 0.080 mmol) was added and stirring was continued for 7 hours longer. The reaction mixture was filtered and purified by preparative HPLC to afford **30** (14 mg, 44%) as a white solid. LCMS *m/z* 459 $[M + H]^+$; ^{1}H NMR (400 MHz, DMSO-d_6) δ ppm 12.35 (brs., 1H), 7.46 (s, 1H), 6.05 (s, 1H), 4.60 (s, 2H), 3.52 (t, *J* = 6.1 Hz, 2H), 3.44 (s, 3H), 2.92 (t, *J* = 6.1 Hz, 2H), 2.32 (s, 3H), 2.20 (s, 3H), 2.04 (brs., 3H), 1.97 (brs., 3H).

5,8-Dichloro-2-((4,6-dimethyl-2-oxo-1,2-dihydropyridin-3-yl)methyl)-7-(3,5-dimethylisoxazol-4-yl)-3,4-dihydroisoquinolin-1(2H)-one (31). To a mixture of 2-((2-(benzyloxy)-4,6-dimethylpyridin-3-yl)methyl)-7-bromo-5,8-dichloro-3,4-dihydroisoquinolin-1(2H)-one, **47** (24 g, 46 mmol), was added 3,5-dimethyl-4-(4,4,5,5-tetramethyl-1,3,2-dioxaborolan-2-yl)isoxazole (15 g, 69 mmol), CsF (21 g, 138 mmol) and tetrakis(triphenylphosphino) palladium(0) ($Pd(PPh_3)_4$, 3.2 g, 2.8 mmol) in anhydrous 1,4-dioxane (600 mL). The mixture was degased with N_2 and heated at 100 °C for 18 h in a sealed tube. The mixture was cooled to room temperature and diluted with EtOAc (250 mL) and H_2O (100 mL). The organic layer was separated and the aqueous layer was extracted with EtOAc (2 x 50 mL).

The organic layers were combined, washed with brine (50 mL), dried over Na_2SO_4 and concentrated *in vacuo* to give the crude intermediate which was purified by column chromatography (petroleum ether/EtOAc = 10:1, R_f = 0.6) to obtain 2-((2-(benzyloxy)-4,6-dimethylpyridin-3-yl)methyl)-5,8-dichloro-7-(3,5-dimethylisoxazol-4-yl)-3,4 dihydroisoquinolin-1(2H)-one (18 g, 73%) as a white solid. This material (18 g, 33 mmol) was then treated with TFA (80 mL) in DCM (30 mL) at room temperature for 12 h. The mixture was concentrated *in vacuo* to give a residue which was basified with saturated aq. $NaHCO_3$ (300 mL) until pH 8. The product was extracted into DCM (3 x 150 mL). The combined organic layers were combined and washed with H_2O (40 mL), brine (40 mL), dried over Na_2SO_4 and concentrated *in vacuo* to give the crude product which was purified by column chromatography (petroleum ether/EtOAc = 1:1, then DCM/MeOH = 20:1, R_f = 0.5 in DCM/MeOH = 10:1). The product was further purified via crystallization from MeOH (50 mL) to obtain **31** (11 g, 74%) as a white solid. LCMS m/z 446 $[M+1]^+$; ^{1}H NMR ($CDCl_3$) δ ppm 12.76 (s, 1H), 7.28 (s, 1H), 5.98 (s, 1H), 4.78 (s, 2H), 3.74 (t, *J* = 6.0 Hz, 2H), 3.00 (t, *J* = 6.0 Hz, 2H), 2.39 (s, 3H), 2.32 (s, 3H), 2.28 (s, 3H), 2.15 (s, 3H).

8-Chloro-2-((4,6-dimethyl-2-oxo-1,2-dihydropyridin-3-yl)methyl)-7-(3,5-dimethylisoxazol-4-yl)-3,4-dihydroisoquinolin-1(2H)-one (32). A 1,4-dioxane (4.0 mL) solution of **50** (124 mg, 0.255 mmol), 3,5-dimethylisoxazole-4-boronic acid pinacol ester (80.1 mg, 0.359 mmol), and cesium fluoride (0.776 mL of 1 M in H_2O, 0.766 mmol) was degassed by bubbling nitrogen through the solution for 20 minutes. The reaction was treated with tetrakis(triphenylphosphino) palladium(0) ($Pd(PPh_3)_4$, 29.8 mg, 0.0258 mmol), sealed, and heated to 100 ^oC using microwave heating for 2 h. The reaction was poured into EtOAc (10 mL) and washed with water (10 mL) and brine (10 mL). The organic layer was concentrated and purified (Biotage SNAP, 10g, HP-

Sil, 0-50% EtOAc in heptane) to give a white gum (78 mg, 61%). LCMS m/z 502 $[M+1]^+$. This intermediate (78 mg, 0.16 mmol) was dissolved in TFA (4.0 mL) and stirred at rt for 4h. The reaction was diluted with heptane and concentrated under vacuum. The resulting residue was purified on reverse phase preparative HPLC to give **32** (64 mg, 49%) as a white solid. LCMS m/z 412 $[M+H]^+$; ^{1}H NMR (700 MHz, DMSO-d_6) δ ppm 7.37 (d, J = 7.5 Hz, 1H), 7.30 (d, J = 7.5 Hz, 1H), 5.94 (s, 1H), 4.56 (s, 2H), 3.42 (t, J = 6.2 Hz, 2H), 2.85 (t, J = 6.2 Hz, 2H), 2.20 (s, 3H), 2.16 (s, 3H), 2.12 (s, 3H), 2.02 (s, 3H).

2-(Benzyloxy)-3-(chloromethyl)-4,6-dimethylpyridine (35b). To a solution of 2-hydroxy-4,6-dimethylpyridine-3-carbonitrile (85.0 g, 0.574 mol) and benzyl chloride (87.0 g, 0.688 mol) in toluene (800 mL) was added Ag_2O (146 g, 0.631 mol). The reaction mixture was stirred at 110 °C overnight. The reaction mixture was filtered through CELITE® and the solids washed with DCM. The filtrate was concentrated under vacuum and purified by column chromatography (petroleum ether/EtOAc) to give 2-(benzyloxy)-4,6-dimethylpyridine-3-carbonitrile (**28a**, 89 g, 65%) as a white solid. To a stirred solution of **34a** (44.5 g, 187 mmol) in DCM (500 mL) was added dropwise DIBAL-H (224 mL of 1M in toluene, 224 mmol) while maintaining the temperature between 0-5 °C during the addition. The reaction mixture was then allowed to warm to room temperature and stirred for an additional 3 hours. The mixture was quenched with 1N HCl (200 mL) and was stirred vigorously for 30 minutes. The reaction was neutralized with 4N NaOH (20 mL) and the biphasic mixture was filtered, and the filtrate washed with DCM (500 mL). The aqueous layer was extracted with DCM (200 mL). The combined organic layers were dried over Na_2SO_4 and concentrated under vacuum. The residue was purified by column chromatography (petroleum ether/EtOAc) to give 2-(benzyloxy)-4,6-dimethylpyridine-3-carbaldehyde (**34b**, 70 g, 78%) as a yellow solid. To a 0 °C solution of **34b** (35.0 g, 145 mmol)

in MeOH (1000 mL) was added $NaBH_4$ (6.60 g, 174 mmol) in portions. The reaction mixture was stirred at room temperature for 2 h. The reaction mixture was concentrated under vacuum and the residue was diluted with saturated aq. $NaHCO_3$. After the bubbling had stopped, the aqueous solution was extracted with EtOAc (2 x 500 mL). The combined organic layers were dried over Na_2SO_4, concentrated under vacuum, and purified by column chromatography (petroleum ether/EtOAc) to give [2-(benzyloxy)-4,6-dimethylpyridin-3-yl]methanol (43 g, 61%) as a colorless oil. To a solution of [2-(benzyloxy)-4,6-dimethylpyridin-3-yl]methanol (21.5 g, 88.5 mmol) in anhydrous DCM (400 mL) was added $SOCl_2$ (16.0 g, 133 mmol) at -40 °C under N_2. The mixture was stirred at the -40 °C for 30 min. The reaction mixture was poured into ice-water (300 mL) and adjusted pH 7-8 with $NaHCO_3$ (solid). The mixture was separated and the aqueous layer was extracted with DCM (300 mL). The combined organic layers were washed with brine (300 mL), dried over Na_2SO_4, and concentrated under vacuum. The residue was purified by column chromatography (petroleum ether/EtOAc, 100:1) to give **35b** (27.5 g, 60%) as a white solid. LCMS *m/z* 262 $[M + H]^+$; ^1H NMR (400 MHz, $CDCl_3$) δ ppm 7.51-7.49 (m, 2H), 7.41-7.37 (m, 2H), 7.34-7.30 (m, 1H), 6.62 (s, 1H), 5.45 (s, 2H), 4.73 (s, 2H), 2.42 (s, 3H), 2.37 (s, 3H).

8-Chloro-7-methoxy-3,4-dihydroisoquinolin-1(2H)-one (38). To a mixture of 7-methoxy-3,4-dihydroisoquinolin-1(2*H*)-one (13.0 g, 73.9 mmol) in conc. H_2SO_4 (120 mL) was added NCS (10.4 g, 77.6 mmol) at 0 ^oC. The reaction mixture was warmed to room temperature and stirred overnight. The reaction mixture was poured onto ice-water (200 mL). The solution was basified with solid Na_2CO_3 to pH 8. The reaction mixture was extracted with EtOAc (2 x 200 mL). The combined organic layers were washed with brine (300 mL), dried over Na_2SO_4 and concentrated under vacuum. The residue was purified by column chromatography (petroleum ether/EtOAc,

1:1) to give 8-chloro-7-methoxy-3,4-dihydroisoquinolin-1(2*H*)-one (**38**, 7.8 g, 50%) as a yellow solid. LCMS m/z 212 $[M + H]^+$; ^1H NMR (400 MHz, DMSO-d_6) δ ppm 8.05 (brs., 1H), 7.18-7.28 (m, 2H), 3.84 (s, 3H), 3.24 (t, J = 6.2 Hz, 2H), 2.80 (t, J = 6.2 Hz, 2H).

8-Chloro-5-fluoro-7-isopropoxy-3,4-dihydroisoquinolin-1(2H)-one (42a). To a mixture of 5-amino-8-chloro-7-isopropoxy-3,4-dihydroisoquinolin-1(2*H*)-one (**41**, 0.500 g, 1.97 mmol) in HBF_4 (10 mL) was added a solution of $NaNO_2$ (204 mg, 2.95 mmol) in H_2O (3.4 mL) at 0 °C. After the addition, the mixture was stirred at 0 °C for 1 h and stirred at room temperature for 1 h. Then, the mixture and heated at 60 °C for 2 h. The mixture was cooled to room temperature and basified with satd. aq. NaOH to pH = 9 and extracted with EtOAc (2 x 20 mL). The combined organic layers were washed with brine (30 mL), dried over Na_2SO_4 and concentrated *in vacuo*. The residue was purified by flash column chromatography (petroleum ether/EtOAc = 1:1, R_f: 0.42) to give **42a** (0.10 g, 20%) as a yellow solid. This compound was used with characterization in the following reactions to synthesize **24**.

5,8-Dichloro-7-isopropoxy-3,4-dihydroisoquinolin-1(2H)-one (42b). A mixture of $CuCl_2$ (270 mg, 2.02 mmol) and LiCl (260 mg, 6.20 mmol) in CH_3CN (15 mL) was stirred at 55 °C for 5 minutes. isoamyl nitrite (110 mg, 0.940 mmol) was added at 55 °C and stirring was continued for 2 minutes. Compound **41** (150 mg, 0.590 mmol) was added and the resulting mixture was stirred at 55 °C for 1 h. The mixture was concentrated to give a residue which was purified by flash chromatography (petroleum ether/EtOAc = 3:1, R_f = 0.3) to give compound **42b** (100 mg, 62%) as a pale yellow solid. LCMS: m/z 274 [M+1]+; 1H NMR (400 MHz, DMSO-d_6) δ ppm 8.22 (brs., 1H), 7.44 (s, 1H), 4.72 (td, J = 6.0, 11.98 Hz, 1H), 3.23-3.30 (m, 2H), 2.86 (t, J = 6.2 Hz, 2H), 1.28 (d, J = 5.9 Hz, 6H).

8-Chloro-5-iodo-7-isopropoxy-3,4-dihydroisoquinolin-1(2H)-one (42c). To a solution of compound **41** (20 g, 78 mmol) and isoamyl nitrite (18 g, 157 mmol) in CH_3CN (80 mL) was added CH_2I_2 (41.1 g, 157 mmol) at room temperature. The resulting mixture was heated at 80 °C for 4 h. TLC (petroleum ether/EtOAc = 3:1, R_f = 0.7) showed the reaction was complete. The mixture was concentrated *in vacuo* to give the crude product, which was purified by column chromatography (on silica gel, petroleum ether/EtOAc = 5:1) to obtain **42c** (13.6 g, 48%) as a yellow solid. LCMS *m/z* 366 $[M+H]^+$; ^1H NMR (400 MHz, $CDCl_3$) δ ppm 7.50 (s, 1H), 6.25 (brs., 1H), 4.55-4.45 (m, 1H), 3.45-3.40 (m, 2H), 3.00-2.95 (m, 2H), 1.40 (s, 3H), 1.38 (s, 3H).

(*R*)-2-((2-(Benzyloxy)-4,6-dimethylpyridin-3-yl)methyl)-8-chloro-5-iodo-7-((tetrahydrofuran-3-yl)oxy)-3,4-dihydroisoquinolin-1(2H)-one (44). Compound **44** was prepared from **43c.** Compound **43c** was prepared from **42c** using a procedure analogous to that described for the synthesis of **40a** but substituting (*S*)-tetrahydrofuran-3-yl methanesulfonate in place of iodoethane. Sodium hydride (60% in oil, 0.74 g, 18.58 mmol) was added in portions to a solution of compound **43c** (3.65 g, 9.29 mmol) in DMF (60 mL) at room temperature under N2 atmosphere. After stirring at room temperature for 30 min, **35b** (2.1 g, 8.36 mmol) was added to the mixture. The resulting mixture was stirred at room temperature for 1 h. TLC (petroleum ether/EtOAc = 1:1) indicated the reaction was complete. The mixture was quenched by H_2O (60 mL) and extracted with EtOAc (2 x 60 mL). The combined organic layers were washed with brine (6 x 60 mL), dried over Na_2SO_4, and concentrated. The residue was purified by Biotage (petroleum ether/EtOAc = 3:1, R_f: 0.36) to give **44** (4.7 g, 81.9%) as a yellow solid. LCMS *m/z* 619 $[M+H]^+$; ^1H NMR (400 MHz, $CDCl_3$) δ ppm 7.45 (m, 2H), 7.35 (m, 3H), 6.67 (s, 1H), 5.43 (s, 2H), 4.86 (m, 1H), 4.75 (s, 2H), 4.12 (m, 4H), 3.82 (m, 1H), 3.25 (m, 2H), 2.61 (m, 2H), 2.41 (s, 3H), 2.32 (s, 3H), 2.23 (m, 2H).

Methyl (2,5-dichlorophenethyl)carbamate (45). To a solution of 2-(2,5-dichlorophenyl)acetonitrile (34.5 g, 185 mmol) in MeOH (1700 mL) was added $NiCl_2 \cdot 6H_2O$ (4.45 g, 18.7 mmol) at 0 °C. After 10 minutes, the solids from the initial green suspension went into solution. Methylchloroformate (38.4 g, 406 mmol) was added via syringe over 10 minutes followed by $NaBH_4$ (41.4 g, 1.09 mol) in eight small portions over 30 minutes at 0 °C. Evolution of gas was observed and the reaction mixture turned black. After the addition was complete, the resulting mixture was stirred at 20 °C for 1 hour. LCMS analysis showed 48% of desired product was detected and 32% of 2-(2,5-dichlorophenyl)ethan-1-amine. Another portion of methylchloroformate (7.7 g, 81 mmol) was added via a syringe at 20 °C. The resulting mixture was stirred at 20 °C for 1 h. The mixture was quenched with H_2O (100 mL) and concentrated to give an off-white residue. The solids were partitioned between EtOAc (1500 mL) and aq. NaOH (1 N, 400 mL). The organic layer was separated and the resulting aqueous suspension layer was filtered. The filtrate was extracted with EtOAc (2 x 300 mL). The organic extracts were combined, washed with brine (150 mL), and dried over Na_2SO_4. Concentration afforded the crude product (40 g), which was purified by column chromatography (petroleum ether/EtOAc = 10:1 to 4:1, R_f = 0.3 in petroleum ether/EtOAc = 10:1) to obtain **45** (25 g, 54%) as a yellow solid. LCMS *m/z* 248 $[M + H]^+$; ^{1}H NMR (400 MHz, DMSO-d_6) δ ppm 7.45 (d, J = 8.6 Hz, 1H), 7.39 (d, J = 2.3 Hz, 1H), 7.32 (dd, J = 2.6, 8.6 Hz, 1H), 7.21 (t, J = 4.3 Hz, 1H), 3.50 (s, 3H), 3.23 (q, J = 6.6 Hz, 2H), 2.83 (t, J = 7.0 Hz, 2H).

5,8-Dichloro-3,4-dihydroisoquinolin-1(2H)-one (46). To methyl (2,5-dichlorophenethyl) carbamate, (**45**, 27.0 g, 109 mmol) in a pre-cooled (0 °C) round bottom flask, was added TfOH (350 mL) dropwise over 30 minutes at 0 °C under a N_2 atmosphere. The yellow suspension was stirred at 10 °C for 20 minutes. After 20 minutes, the mixture dissolved to form a yellow

solution which was heated at 80 °C for 12 hours. The mixture was then poured into 1500 g of crushed ice. The resulting white precipitate was filtered and filter cake set aside. The filtrate was extracted with DCM (3 x 500 mL). Then, the white filtrate was dissolved in the extract. The combined organic extract was washed with 1N NaOH (200 mL), brine (100 mL), and then dried over Na_2SO_4. Concentration gave the crude product (30 g), which was stirred in a mixture of petroleum ether (125 mL) and EtOAc (25 mL) for 30 minutes. The suspension was filtered and the cake was dried *in vacuo* to give **46** (17 g, 72%) as a yellow solid. LCMS *m/z* 216 $[M + H]^+$; ^{1}H NMR (400 MHz, DMSO-d_6) δ ppm 8.23 (brs., 1H), 7.59 (d, J = 8.6 Hz, 1H), 7.43 (d, J = 8.6 Hz, 1H), 3.26-3.36 (m, 2H), 2.96 (t, J = 6.4 Hz, 2H).

2-((2-(Benzyloxy)-4,6-dimethylpyridin-3-yl)methyl)-7-bromo-5,8-dichloro-3,4-dihydroisoquinolin-1(2H)-one (47). A suspension of 5,8-dichloro-3,4-dihydroisoquinolin-1(2H)-one, **46** (50.4 g, 233 mmol) in conc. H_2SO_4 (425 mL, c = 0.549 M) was heated to 45 °C until it became homogeneous. Then, the solution was cooled to 0 °C prior to adding NBS (46.0 g, 256 mmol). The ice bath was removed and the reaction was heated at 45 °C for 4h. The reaction was then cooled to room temperature and poured over crushed ice (200 g). The precipitate that formed was collected by filtration, washed with water (5 x 100 mL), and dried in a vacuum oven at 65 °C for 3 days to give 7-bromo-5,8-dichloro-3,4-dihydroisoquinolin-1(2H)-one (68 g, 99%) as a yellow powder. LCMS *m/z* 294 $[M + H]^+$; ^{1}H NMR (400 MHz, DMSO-*d*6) δ ppm 7.16 (s, 1H), 2.62 (t, J = 6.4 Hz, 2H), 2.22 (t, J = 6.4 Hz, 2H). To a solution of 7-bromo-5,8-dichloro-3,4-dihydroisoquinolin-1(2H)-one (1.00 g, 3.39 mmol) in anhydrous DMF (15 mL) at 0 °C was added KOt-Bu (3.73 mL of 1 M in THF, 3.73 mmol) dropwise. After stirring this mixture for 30 min., **35b** (976 mg, 3.73 mmol) was added. The resulting mixture was stirred at 0 °C for 30 min. The reaction mixture was partitioned between ethyl acetate (100 mL) and water

(100 mL). The organic phase was separated, washed with water (1 x 100 mL) and brine (1 x 100 mL), dried over sodium sulfate, concentrated to dryness, and purified by flash chromatography with a gradient elution of 0-40% EtOAc/Heptane to afford **47** (747 mg, 85%). LCMS *m/z* 519 $[M + H]^+$; ^{1}H NMR (400 MHz, DMSO-d_6) δ ppm 8.07 (s, 1H), 7.40-7.45 (m, 2H), 7.25-7.33 (m, 3H), 6.75 (s, 1H), 5.37 (s, 2H), 4.70 (s, 2H), 3.24 (t, *J* = 6.2 Hz, 2H), 2.71 (t, *J* = 6.2 Hz, 2H), 2.35 (s, 3H), 2.30 (s, 3H).

2-(2-Benzyloxy-4,6-dimethyl-pyridin-3-ylmethyl)-5,8-dichloro-7-[3-methyl-1-(tetrahydro-pyran-2-yl)-1H-pyrazol-4-yl]-3,4-dihydro-2H-isoquinolin-1-one (48). 2-(2-Benzyloxy-4,6-dimethyl-pyridin-3-ylmethyl)-7-bromo-5,8-dichloro-3,4-dihydro-2H-isoquinolin-1-one (**47**) (150 mg, 0.29 mmol), 4,4,4',4',5,5,5',5'-octamethyl-2,2'-bi(1,3,2-dioxaborolane) (148 mg, 0.58 mmol), 1,1'-bis(diphenylphosphino)ferrocene palladium dichloride ($Pd(dppf)Cl_2$, 8 mg, 0.01 mmol), potassium acetate (85 mg, 0.87 mmol) and dioxane (1.9 mL) were sequentially added to a microwave vial. The vial was sealed, degassed, purged with nitrogen and placed in a sand bath at 65 ^{o}C and warmed to 95 ^{o}C which gave an amber solution. After two hours, LCMS gave a mixture of the aryl boronate ester and acid, and unreacted aryl bromide. Thus, more catalyst (4 mg, 0.005 mmol) and 4,4,4',4',5,5,5',5'-octamethyl-2,2'-bi(1,3,2-dioxaborolane) (38 mg) were added to the black reaction mixture. After one hour, LCMS gave product and no starting material. Next, the reaction was cooled to room temperature followed by the sequential addition of 4-bromo-5-methyl-1-(tetrahydro-pyran-2-yl)-1H-pyrazole (141 mg, 0.58 mmol), aq. Na_2CO_3 (2 M, 0.72 mL, 1.45 mmol) and $Pd(dppf)Cl_2$ (7 mg, 0.01 mmol). The biphasic reaction mixture was placed in a sand bath at 95 ^{o}C. After 2 h, LCMS gave the desired product and no boronic acid or boronate ester. The reaction was cooled to room temperature and diluted with ethyl acetate. The layers were separated and the aqueous layer was extracted with ethyl acetate. The

combined organic layers were washed with water, brine, dried over $MgSO_4$, and filtered through a silica plug which was eluted with 10% methanol-ethyl acetate. The filtrate was concentrated under reduced pressure which gave a brown oil. TLC (40% ethyl acetate-heptane) gave R_f 0.8, R_f 0.4 and R_f 0.0. The crude product was purified over silica (2 mm chromatotron plate) which was eluted with 5-40% ethyl acetate-heptane and gave **48** as a colorless oil (27 mg, 15% yield). TLC (40% ethyl acetate-heptane): R_f 0.4; LCMS *m/z* 606 $[M+1]^+$; ^1H NMR (400 MHz, CD_3OD-d_4) δ 7.83 (s, 1H), 7.47 (s, 1H), 7.42-7.45 (m, 2H), 7.24-7.31 (m, 3H), 6.74 (s, 1H), 5.45 (s, 2H), 5.32-5.43 (dd, *J* = 2.2, 9.9 Hz, 1H), 4.86 (s, 2H), 4.06-4.09 (m, 1H), 3.73-3.78 (m, 1H), 3.29 (t, *J* = 6.3 Hz, 2H), 2.79 (t, *J* = 6.2 Hz, 2H), 2.42 (s, 3H), 2.38 (s, 3H), 2.18 (s, 3H), 2.06 (brs., 2H), 1.56-1.88 (m, 4H).

7-Amino-8-chloro-3,4-dihydroisoquinolin-1(2H)-one (49). To a solution of commercially available 7-amino-3,4-dihydroisoquinolin-1(2H)-one (401 mg, 2.47 mmol) in DMF (10 mL) was added NCS (310 mg, 2.32 mmol) and the reaction was heated to 55 ^oC for 7 h. The reaction was diluted with EtOAc and washed with water. The water layer was extracted with EtOAc and the combined organic layers were concentrated and purified on reverse phase prep-HPLC to give **49** (189 mg, 39%). LCMS m/z 197 $[M+H]^+$; ^1H NMR (400 MHz, DMSO-d_6) δ ppm 7.88 (brs., 1H), 6.96 (d, *J* = 8.2 Hz, 1H), 6.88 (d, *J* = 8.1 Hz, 1H), 5.33 (s, 2H), 3.21 (dt, *J* = 3.8, 6.2 Hz, 2H), 2.70 (t, *J* = 6.2 Hz, 2H).

2-((2-(Benzyloxy)-4,6-dimethylpyridin-3-yl)methyl)-7-bromo-8-chloro-3,4-dihydroisoquinolin-1(2H)-one (50). Copper(I) bromide (282 mg, 1.97 mmol) in acetonitrile (7.0 mL) was stirred at 60 ^oC for 10 minutes. To this was added isoamyl nitrite (84 mg, 0.72 mmol) followed by **49** (129 mg, 0.656 mmol). The reaction mixture was stirred at 60 ^oC for 1 h. The reaction was cooled to room temperature and stirred vigorously with saturated aq. NH_4Cl

(10 mL) for 30 minutes. The biphasic mixture was diluted with EtOAc and water, and the layers were separated. The organic layer was washed with brine and concentrated. The resulting oil was purified on silica gel (Biotage SNAP, HP-Sil, 10g, 40-90% EtOAc in DCM) to give 7-bromo-3,4-dihydroisoquinolin-1(2H)-one (65 mg, 38%) as a yellow powder. LCMS m/z 260, 262 $[M+H]^+$; ^{1}H NMR (400 MHz, $CDCl_3$-*d*) δ 7.70 (d, *J* = 8.3 Hz, 1H), 7.03 (d, *J* = 8.1 Hz, 1H), 6.07 (brs., 1H), 3.49 (td, *J* = 3.0, 5.93 Hz, 2H), 2.96 (t, *J* = 6.2 Hz, 2H). To a solution 7-bromo-3,4-dihydroisoquinolin-1(2H)-one (87.2 mg, 0.335 mmol) in DMF (4.0 mL) at 0 ^{o}C was added potassium *t*-butoxide (0.40 mL of 1 M in THF, 0.40 mmol). After 5 minutes, **35b** (92.0 mg, 0.351 mmol) was added in one portion and stirred at 0 ^{o}C for 0.5 h. The reaction was quenched with AcOH (3 drops), diluted with MTBE and washed with water (2 x 10 mL). The organic layer was concentrated and the resulting oil was purified on silica gel (Biotage SNAP, 10 g, 0-25% EtOAc in heptane) to give **50** (126 mg, 78%) as a gum. LCMS m/z 485, 487 $[M+H]^+$; ^{1}H NMR (400 MHz, $CDCl_3$-*d*) δ ppm 7.63 (d, *J* = 8.1 Hz, 1H), 7.44-7.49 (m, 2H), 7.31-7.39 (m, 3H), 6.90 (d, *J* = 8.1 Hz, 1H), 6.71 (s, 1H), 5.62 (s, 2H), 4.86 (s, 2H), 3.23-3.28 (m, 2H), 2.64 (t, *J* = 5.9 Hz, 2H), 2.56 (s, 3H), 2.41 (s, 3H).

2-(((2-(Benzyloxy)-4,6-dimethylpyridin-3-yl)methyl)amino)ethan-1-ol (52). To a suspension of **34b** (6.4 g, 27 mmol) in methanol (100 mL) was added 2-aminoethanol (8.34 mL, 133 mmol). The reaction mixture was stirred at room temperature for 1 h and cooled to 0 °C. Sodium cyanoborohydride (4.9 g, 66 mmol) was added in one portion and the reaction was slowly warmed to room temperature and stirred for 16 h. The methanol was removed under vacuum then the residue was diluted with water (50 mL) and extracted with DCM (2 x 50 mL). The combined organic extracts were dried over $MgSO_4$, concentrated under vacuum and purified by column chromatography (100% EtOAc) to give **52** (4.2 g, 55%) as a pale yellow solid. LCMS

m/z 287 [M + H]+; ^{1}H NMR (400 MHz, DMSO-d_6) δ ppm 7.46 (d, J = 7.1 Hz, 2H), 7.37 (t, J = 7.3 Hz, 2 H), 7.26 - 7.33 (m, 1H), 6.68 (s, 1 H), 5.33 (s, 2H), 4.41 (t, J = 5.2 Hz, 1H), 3.69 (s, 2H), 3.41 (q, J = 5.4 Hz, 2H), 3.32 (s, 1H), 2.52 - 2.57 (m, 2H), 2.31 (s, 3H), 2.28 (s, 3H).

Determination of compound off-rates and residence time

PRC2 4-complex (0.4 mg/mL; EZH2, SUZ12, EED, RbAp48) was incubated with 0.4 μM compound in 100 mM Tris pH 8.5, 4 mM DTT for 20 minutes. Measurement of compound dissociation was initiated by addition of 100-fold excess of a competing compound to prevent re-binding. At the indicated time points, dissociated compound was separated from enzyme bound compound by transferring to a pre-equilibrated 0.5 mL Zeba desalting column (7K MWCO). Eluents containing the PRC2-compound complex were transferred into a 96-well plate, where 1% formic acid was added to aid in the analysis by mass spectrometry. Excess compound **32** was used to compete off compound **31** and compound **1**[46], while excess **31** was used to compete off **32**. 100% occupancy was determined by taking a sample prior to addition of the competitor compound, and 0% occupancy was determined by adding the excess competitor compound prior to the compound of interest and then transferring to the desalting column. Compound quantification was carried out using a RapidFire 350 high-throughput solid phase extraction chromatography system coupled to an Agilent 6550 quadrupole-time of flight (Q-TOF) mass spectrometer. Reaction mixture (42 μL) was injected onto an Agilent Graphite Type D cartridge in 0.1% TFA and eluted in 80% acetonitrile and 0.1% TFA. The RapidFire settings were as follows: 600 ms (or until loop was full as detected via sip sensor) aspiration time, 3,000 ms load time, 6,000 ms elution time, 500 ms re-equilibration time, 1.5 mL/min flow rate for pump A, 1.25 mL/min flow rate for pump B, and 1.25 mL/min flow rate for pump C.

After elution, samples were analyzed on an Agilent 6550 Q-TOF mass spectrometer with an Agilent Jet Stream source with ion funnel technology, set in positive ion mode. Mass spectrometry settings were as follows: 225 degree Celsius gas temperature, 17 L/min drying gas, 50 psig nebulizer, 250 degree Celsius sheath gas temperature, 9 L/min sheath gas flow rate, 3500 V capillary voltage, 1000 V nozzle voltage, 350 V fragmentor, 65 V skimmer, 750 V OCT 1 RF Vpp.

Peaks were analyzed in RapidFire Integrator software by extracting ion chromatograms for the compounds using the following m/z values: 446.1033 m/z for compound **31**, 527.3129 m/z for compound **1**, and 412.1422 m/z for compound **32**. Integrated peak data was then converted into %occupancy using the 100% and 0% occupancy standards. Finally, %occupancy data was fit to a one-phase exponential decay equation (Y=(Y0 - Plateau)*exp(-k*X) + Plateau) using Prism 6 (GraphPad Software). k approximates k_{off} and residence time is calculated as 1/k.

Cell culture

Human B-cell non-Hodgkin lymphoma cell line Karpas-422 was obtained from Deutsche Sammlung von Mikroorganismen und Zellkulturen (DSMZ) in Germany, Cat. ACC-32. Cells were cultured in RPMI 1640 plus 10-20% (v/v) FBS and 1% Pen/Strep.

H3K27Me3 ELISA Assay

Karpas-422 cells were plated in complete cell culture medium (100 μL/well) in a 96-well clear, V bottom polystyrene cell culture plate (Costar, Cat 3894) at a density of 2,500 cells/well. Cells were then incubated for 2 to 3 hours at 37 ^{o}C and 5% CO_2. Compound dilution plates were prepared in 96-well, clear U-bottom, polypropylene plates (Corning, Cat. 3365) in 100% DMSO

at 10 mM stock concentration in duplicate wells, using an 11-point serial dilution (1:3 dilutions). Compounds were further diluted in growth medium and 25 μL were added to each well of the cell plates using a Beckman FX liquid handling system such that the highest compound concentration tested was 50 μM final, with a 0.5% final DMSO concentration. Plates were then incubated for 72 hours at 37 ^{o}C and 5% CO_2. At the end of the incubation period with compound, plates were centrifuged at 2000 rpm for 5 minutes at room temperature and medium was removed. Then, 100 μL acid extracted solution was added to each well. Plates were shaken for 50 minutes at 4 ^{o}C to lyse cells and then 38 μL of neutralization buffer was added. Plates were then frozen at -80 ^{o}C. The next day, plates were shaken at room temperature to thaw. Cell lysates (50 μL/well) were then transferred to ELISA plates. Plates were covered and incubated for 2.5 hours at room temperature, with constant slow speed shaking. After incubation, plates were washed seven times (300 μL/well) with 1x Wash Buffer using a BioTek plate washer. Then 100 μL of Biotinylated Tri-methyl Histone H3K27 detection antibody was added to each well and incubated for 2 hours at room temperature with constant slow speed shaking. After incubation, plates were washed as described. One hundred μL of HRP-linked antibody was added to each well and incubated for 60 minutes at room temperature with constant slow speed shaking. After incubation, plates were washed as described. Finally, 100 μL of TMB substrate reagent was added to each well and incubated for 5 minutes at room temperature in the dark with slow shaking and 100 μL of Stop Solution was added to stop the reaction. Plates were read on the PerkinElmer Envision plate reader using the 96-well with OD reading mode. IC_{50} values were calculated using a four-parameter fit with GraphPad Prism or in house modified IDBS ActivityBase data analyzing package.

Cell growth inhibition assay

Karpas-422 cells were plated in complete cell culture medium (100µL/well) in a 96-well clear, flat bottom polystyrene cell culture plate (Greiner, Cat. 655182) at a density of 2,000 cells/well. Cells were then incubated for 2 to 3 hours at 37 ^{o}C and 5% CO_2. Compound dilution plates were prepared and compounds were further diluted in growth medium as described above. Then, 25 µL of the diluted compound was added to each well of the cell plates using a Beckman FX liquid handling system. Plates were then incubated for 72 hours at 37 ^{o}C and 5% CO_2. At the end of the incubation period with compound, compounds were again diluted in growth medium and 30 µL were added to each well of the cell plates using a Beckman FX liquid handling system. Plates were then incubated for 96 hours at 37 ^{o}C and 5% CO_2. At the end of the incubation period, plates were centrifuged at 2000 rpm for 5 minutes at room temperature and medium was removed. Then 100 µL of fresh complete cell culture medium was added to each well. Compounds were once more diluted in growth medium and 25 µL were added to each well of the cell plates using a Beckman FX liquid handling system. Plates were then incubated for 72 hours at 37 ^{o}C and 5% CO_2. After the incubation period, plates were centrifuged at 2000 rpm for 5 minutes at room temperature and medium was removed. Then 100 µL of fresh complete cell culture medium was added to each well. Finally, rezasurin in PBS (1 mg/mL) was added to each well of the cell plate (15 µL/well). The plates were incubated at 37 ^{o}C and 5% CO_2 for 6 hours in the dark. Plates were read on the PerkinElmer Envision plate reader using the 96-well with fluorescent reading mode at 530 nm excitation and 590 nm emissions. IC_{50} values were calculated using a four-parameter fit with GraphPad Prism or in house modified IDBS ActivityBase data analyzing package.

Pharmacokinetics

Microsomal Stability Studies

Compounds (1 μM) were incubated at 37 °C for 45 min in a final volume of 200 μL of 100 mM potassium phosphate buffer (pH 7.4) containing pooled liver microsomes (0.8 mg/ml protein) and 2 mM NADPH. Reactions were initiated with the addition of NADPH following a 10-min pre-incubation. Aliquots of incubation samples were protein precipitated with cold methanol containing 0.1 μM buspirone (internal standard) and centrifuged, and supernatants were analyzed by LC-MS/MS. All incubations were performed in triplicate. In vitro intrinsic clearance (CL_{int}) was calculated from half-life ($t_{1/2}$) of the parent drug disappearance, which was determined by the slope (k) of log-linear regression analysis from the concentration versus time profiles, i.e., $t_{1/2} = -\ln(2)/k$.

Efficacy study in Karpas-422 Xenograft model

Animals. Female Scid beige mice (6-8 weeks old) were obtained from Charles River. Animals were maintained under clean room conditions in sterile filter top cages with Alpha-Dri bedding and housed on high efficiency particulate air–filtered ventilated racks. Animals received sterile rodent chow and water ad libitum. All of the procedures were conducted in accordance with the Institute for Laboratory Animal Research Guide for the Care and Use of Laboratory Animals and with Pfizer Animal Care and Use Committee guidelines.

To generate subcutaneous xenograft model, Karpas-422 cells (5 million cells/animal) in 100 μL medium were mixed with equal volume of Matrigel and implanted in the flank of female SCID beige mice. When tumors reached the average size of 200 mm^3, tumor-bearing animals were randomized into treatment groups: vehicle, compound **31** at 200 mg/kg and 300 mg/kg.

Compound **25** was formulated in 0.5% NaCMC and 0.1% Tween 80, at final pH 4.5. All treatments were given BID for 20 days, and tumor volume was calculated based on two-dimensional measurement every 3-5 days throughout the study. A subset of the tumors and plasma were harvested on day 11 and day 20 (1 and 4 h post treatment) for ex vivo PD biomarker analysis (methods in supplementary material). Additionally, plasma samples were collected at 0.5, 2, 4, 6, 8 and 24 h post treatment on day 20. After the final dosing on day 20, the remaining tumor bearing animals that were not terminated for PD purpose were continuously monitored for additional 3 weeks (for additional 50 days following cessation of treatment).

ASSOCIATED CONTENT

Supporting Information

Enzymatic assay, biology experimental details, computational method, ITC method, and compound analytical data are provided. This material is available free of charge via the internet at http://pubs.acs.org.

AUTHOR INFORMATION

Corresponding Author

E-mail: peipei.kung@pfizer.com. Phone: (858) 526-4867.

ACKNOWLEDGMENTS

We are grateful to Drs. Ted W. Johnson and Rob Kania for helpful discussions during manuscript preparation. We also acknowledge Jeff Elleraas, Loanne Chung, and Phuong Tran for purification assistance.

ABBREVIATIONS USED

HOAc: acetic acid; EtOAc, ethyl acetate; RuPhos, 2-dicyclohexylphosphino-2,6-diisopropoxybiphenyl; TfOH, trifluoromethanesulfonic acid; DIEA, diisopropyl ethyl amine; CEREP, Eurofins Cerep SA.

REFERENCES AND NOTES

1. Jones, P. A.; Baylin, S. B. The fundamental role of epigenetic events in cancer. *Nat. Rev. Genet.* **2002**, *3*, 415-428.
2. Egger, G.; Liang, G.; Aparicio A; Jones, P. A. Epigenetics in human disease and prospects for epigenetic therapy. *Nature* **2004**, *429*, 457-463.
3. Chuang, J. C.; Jones, P. A. Epigenetics and microRNAs. *Pediatr. Res.* **2007**, *61*, 24R-29R.
4. (a) Timp, W.; Feinberg, A. P. Cancer as a dysregulated epigenome allowing cellular growth advantage at the expense of the host. *Nat. Rev. Cancer* **2013**, *13*, 497-510. (b) Berdasco, M.; Esteller, M., Aberrant epigenetic landscape in cancer: how cellular identity goes awry. *Dev. Cell* **2010,** *19*, 698-711.
5. Martin, C.; Zhang, Y. The diverse functions of histone lysine methylation. *Nat. Rev. Mol. Cell Biol.* **2005**, *6*, 838-849.
6. Ezponda, T.; Licht, J. D. Molecular pathways: deregulation of histone H3 Lysine 27 methylation in cancer-different paths, same destination. *Clin. Cancer Res.* **2014**, *20*, 5001-5008.
7. (a) Copeland, R. A.; Solomon, M. E.; Richon, V. M. Protein methyltransferases as a target class for drug discovery. *Nat. Rev. Drug Discovery* **2009**, *8*, 724-732. (b) Dawson, M. A.; Kouzarides, T. Cancer epigenetics: from mechanism to therapy. *Cell* **2012,** *150*,

12-27. (c) Helin, K.; Dhanak, D. Chromatin proteins and modifications as drug targets. *Nature* **2013,** *502*, 480-488.

8. Margueron, R.; Reinberg, D, The Polycomb complex PRC2 and its mark in life. *Nature* **2011,** *469*, 343-349.
9. Bracken, A. P.; Helin, K. Polycomb group proteins: navigators of lineage pathways led astray in cancer. *Nat. Rev. Cancer* **2009**, *9*, 773-784.
10. Morin, R. D.; Johnson, N. A.; Severson, T. M.; Mungall, A. J.; An, J.; Goya, R.; Paul, J. E.; Boyle, M.; Woolcock, B. W.; Kuchenbauer, F.; Yap, D.; Humphries, R. K.; Griffith, O. L.; Shah, S.; Zhu, H.; Kimbara, M.; Shashkin, P.; Charlot, J. F.; Tcherpakov, M.; Corbett, R.; Tam, A.; Varhol, R.; Smailus, D.; Moksa, M.; Zhao, Y.; Delaney, A.; Qian, H.; Birol, I.; Schein, J.; Moore, R.; Holt, R.; Horsman, D. E.; Connors, J. M.; Jones, S.; Aparicio, S.; Hirst, M.; Gascoyne, R. D.; Marra, M. A. Somatic mutations altering EZH2 (Tyr641) in follicular and diffuse large B-cell lymphomas of germinal-center origin. *Nat. Genet.* **2010,** *42*, 181-185.
11. Morin, R. D.; Mendez-Lago, M.; Mungall, A. J.; Goya, R.; Mungall, K. L.; Corbett, R. D.; Johnson, N. A.; Severson, T. M.; Chiu, R.; Field, M.; Jackman, S.; Krzywinski, M.; Scott, D. W.; Trinh, D. L.; Tamura-Wells, J.; Li, S.; Firme, M. R.; Rogic, S.; Griffith, M.; Chan, S.; Yakovenko, O.; Meyer, I. M.; Zhao, E. Y.; Smailus, D.; Moksa, M.; Chittaranjan, S.; Rimsza, L.; Brooks-Wilson, A.; Spinelli, J. J.; Ben-Neriah, S.; Meissner, B.; Woolcock, B.; Boyle, M.; McDonald, H.; Tam, A.; Zhao, Y.; Delaney, A.; Zeng, T.; Tse, K.; Butterfield, Y.; Birol, I.; Holt, R.; Schein, J.; Horsman, D. E.; Moore, R.; Jones, S. J.; Connors, J. M.; Hirst, M.; Gascoyne, R. D.; Marra, M. A. Frequent mutation of histone-modifying genes in non-Hodgkin lymphoma. *Nature* **2011,** *476*, 298-303.

12. McCabe, M. T.; Graves, A. P.; Ganji, G.; Diaz, E.; Halsey, W. S.; Jiang, Y.; Smitheman, K. N.; Ott, H. M.; Pappalardi, M. B.; Allen, K. E.; Chen, S. B.; Della Pietra, A., 3rd; Dul, E.; Hughes, A. M.; Gilbert, S. A.; Thrall, S. H.; Tummino, P. J.; Kruger, R. G.; Brandt, M.; Schwartz, B.; Creasy, C. L. Mutation of A677 in histone methyltransferase EZH2 in human B-cell lymphoma promotes hypertrimethylation of histone H3 on lysine 27 (H3K27). *Proc. Nat. Acad. Sci. U.S.A.* **2012,** *109*, 2989-2994.

13. Sneeringer, C. J.; Scott, M. P.; Kuntz, K. W.; Knutson, S. K.; Pollock, R. M.; Richon, V. M.; Copeland, R. A. Coordinated activities of wild-type plus mutant EZH2 drive tumor-associated hypertrimethylation of lysine 27 on histone H3 (H3K27) in human B-cell lymphomas. *Proc. Nat. Acad. Sci. U.S.A.* **2010,** *107*, 20980-20985.

14. McCabe, M. T.; Ott, H. M.; Ganji, G.; Korenchuk, S.; Thompson, C.; Van Aller, G. S.; Liu, Y.; Graves, A. P.; Pietra, A. D.; Diaz, E.; LaFrance, L. V.; Mellinger, M.; Duquenne, C.; Tian, X.; Kruger, R. G.; McHugh, C. F.; Brandt, M.; Miller, W. H.; Dhanak, D.; Verma, S. K.; Tummino, P. J.; Creasy, C. L. EZH2 inhibition as a therapeutic strategy for lymphoma with EZH2-activating mutations. *Nature* **2012**, *492*, 108-112.

15. Knutson, S. K.; Kawano, S.; Minoshima, Y.; Warholic, N. W.; Huang, K.-C.; Xiao, Y.; Kadowaki, T.; Uesugi, M.; Kuznetsov, G.; Kumar, N.; Wigle, T. J.; Klaus, C. R.; Allain, C. J.; Raimondi, A.; Waters, N. J.; Simth, J. J.; Porter-Scott, M.; Chesworth, R.; Moyer, M. P.; Copeland, R. A.; Richon, V. M.; Uenaka, T.; Pollock, R. M.; Kuntz, K. W.; Yokoi, A.; Keilhack, H. Selective inhibition of EZH2 by EPZ-6438 leads to potent antitumor activity in EZH2-mutant non-hodgkin lymphoma. *Mol. Cancer Ther.* **2014**, *13*, 842-854.

16. Konze, K. D.; Ma, A.; Li, F.; Barsyte-Lovejoy, D.; Parton, T.; Macnevin, C. J.; Liu, F.; Gao, C.; Huang, X. P.; Kuznetsova, E.; Rougie, M.; Jiang, A.; Pattenden, S. G.; Norris, J. L.; James, L. I.; Roth, B. L.; Brown, P. J.; Frye, S. V.; Arrowsmith, C. H.; Hahn, K. M.; Wang, G. G.; Vedadi, M.; Jin, J. An orally bioavailable chemical probe of the Lysine Methyltransferases EZH2 and EZH1. *ACS Chem. Biol.* **2013,** *8*, 1324-1334.

17. Qi, W.; Chan, H.; Teng, L.; Li, L.; Chuai, S.; Zhang, R.; Zeng, J.; Li, M.; Fan, H.; Lin, Y.; Gu, J.; Ardayfio, O.; Zhang, J. H.; Yan, X.; Fang, J.; Mi, Y.; Zhang, M.; Zhou, T.; Feng, G.; Chen, Z.; Li, G.; Yang, T.; Zhao, K.; Liu, X.; Yu, Z.; Lu, C. X.; Atadja, P.; Li, E. Selective inhibition of Ezh2 by a small molecule inhibitor blocks tumor cells proliferation. *Proc. Nat. Acad. Sci. U.S.A.* **2012**, *109*, 21360-21365.

18. Gehling, V. S.; Vaswani, R. G.; Nasveschuk, C. G.; Duplessis, M.; Iyer, P.; Balasubramanian, S.; Zhao, F.; Good, A. C.; Campbell, R.; Lee, C.; Dakin, L. A.; Cook, A. S.; Gagnon, A.; Harmange, J. C.; Audia, J. E.; Cummings, R. T.; Normant, E.; Trojer, P.; Albrecht, B. K. Discovery, design, and synthesis of indole-based EZH2 inhibitors. *Bioorg. Med. Chem. Lett.* **2015**, *25*, 3644-3649.

19. Knutson, S. K.; Warholic, N. M.; Wigle, T. J.; Klaus, C. R.; Allain, C. J.; Raimondi, A.; Porter Scott, M.; Chesworth, R.; Moyer, M. P.; Copeland, R. A.; Richon, V. M.; Pollock, R. M.; Kuntz, K. W.; Keilhack, H. Durable tumor regression in genetically altered malignant rhabdoid tumors by inhibition of methyltransferase EZH2. *Proc. Nat. Acad. Sci. U.S.A.* **2013,** *110*, 7922-7927.

20. Wilson, B. G.; Roberts, C. W. SWI/SNF nucleosome remodellers and cancer. *Nat. Rev. Cancer* **2011,** *11*, 481-492.

21. Ginn, K. F.; Gajjar, A. Atypical teratoid rhabdoid tumor: current therapy and future directions. *Front. Oncol.* **2012,** *2*, 114.

22. Bitler, B. G.; Aird, K. M.; Garipov, A.; Li, H.; Amatangelo, M.; Kossenkov, A. V.; Schultz, D. C.; Liu, Q.; Shih Ie, M.; Conejo-Garcia, J. R.; Speicher, D. W.; Zhang, R. Synthetic lethality by targeting EZH2 methyltransferase activity in ARID1A-mutated cancers. *Nat. Med.* **2015,** *21*, 231-238.

23. Lovering, F.; Bikker, J.; Humblet, C. Escape from flatland: increasing saturation as an approach to improving clinical success. *J. Med. Chem.* **2009**, *52*, 6752-6756.

24. Epizyme press release (corporate update) in October, 2015: http://www.epizyme.com/

25. Young, R. J. Physical properties in drug design. *Top. Med. Chem.* **2015**, *9*, 1-68.

26. An independent study of the benzamide carbonyl torsional angle was recently published while we are preparing this manuscript: Kuntz, K. W.; Campbell, J. E.; Keilhack, H.; Pollock, R. M.; Knutson, S. K.; Porter-Scott, M.; Richon, V. M.; Sneeringer, C. J.; Wigle, T. J.; Allain, C. J.; Majer, C. R.; Moyer, M. P.; Copeland, R. A.; Chesworth, R. The Importance of Being Me: Magic methyls, methyltransferase inhibitors, and the discovery of Tazemetostat. *J. Med. Chem.* **2016,** *59*, 1556-1564.

27. Stepan, A. F.; Kauffman, G. W.; Keefer, C. E.; Verhoest, P. R.; Edwards, M. P. Evaluating the differences in cycloalkyl ether metabolism using the design parameter "lipophilic metabolism efficiency" (LipMetE) and a matched molecular pairs analysis. *J. Med. Chem.* **2013**, *56*, 6985-6990.

28. A recently published co-crystal structure of a closely-related analog of 26 provides some insight.[29] In this structure, the carbonyl oxygen adopts a torsion angle of approximately -34° and was reported to form a hydrogen bond with the backbone N-H of Tyr111 that is

located approximately 70° below the plane of the aromatic ring. The geometry of this hydrogen bond is observed to be sub-optimal[30] despite the fact that the carbonyl oxygen is rotated significantly more than the 20° expected based on the quantum density functional calculations. Consistent with our hypothesis, a greater, strain-free rotation of the carbonyl torsion angle is expected to result in an improved hydrogen-bond geometry leading to a more favorable hydrogen bond energy.

29. Brooun, A.; Gajiwala, K. S.; Deng, Y. L.; Liu, W.; Bolanos, B.; Bingham, P.; He, Y. A.; Diehl, W.; Grable, N.; Kung, P. P.; Sutton, S.; Maegley, K. A.; Yu, X.; Stewart, A. E. Polycomb repressive complex 2 structure with inhibitor reveals a mechanism of activation and drug resistance. *Nat. Commun.* **2016,** *7*, 11384.

30. Taylor, R.; Kennard, O. Hydrogen-bond geometry in organic crystals. *Acc. Chem. Res.* **1984**, *17*, 320-326.

31. Ladbury, J. E.; Klebe, G.; Freire, E. Adding calorimetric data to decision making in lead discovery: a hot tip. *Nat. Rev. Drug Discovery* **2010,** *9*, 23-27.

32. Chaires, J. B. Calorimetry and thermodynamics in drug design. *Annu. Rev. Biophys.* **2008**, *37*, 135-151.

33. Olsson, T. S.; Ladbury, J. E.; Pitt, W. R.; Williams, M. A. Extent of enthalpy-entropy compensation in protein-ligand interactions. *Protein Sci.* **2011,** *20*, 1607-1618.

34. Snyder, P. W.; Mecinovic, J.; Moustakas, D. T.; Thomas, S. W., 3rd; Harder, M.; Mack, E. T.; Lockett, M. R.; Heroux, A.; Sherman, W.; Whitesides, G. M. Mechanism of the hydrophobic effect in the biomolecular recognition of arylsulfonamides by carbonic anhydrase. *Proc. Nat. Acad. Sci. U.S.A.* **2011,** *108*, 17889-17894.

35. Di, L.; Whitney-Pickett, C.; Umland, J. P.; Zhang, H.; Zhang, X.; Gebhard, D. F.; Lai, Y.; Federico, J. J., 3rd; Davidson, R. E.; Smith, R.; Reyner, E. L.; Lee, C.; Feng, B.; Rotter, C.; Varma, M. V.; Kempshall, S.; Fenner, K.; El-Kattan, A. F.; Liston, T. E.; Troutman, M. D. Development of a new permeability assay using low-efflux MDCKII cells. *J. Pharm. Sci.* **2011,** *100*, 4974-4985.

36. (a) Leeson, P. D.; Springthorpe, B. The influence of drug-like concepts on decision-making in medicinal chemistry. *Nat. Rev. Drug Discovery* **2007,** *6* , 881-890;

(b) Ryckmans, T.; Edwards, M. P.; Horne, V. A.; Correia, A. M.; Owen, D. R.; Thompson, L. R.; Tran, I.; Tutt, M. F.; Young, T. Rapid assessment of a novel series of selective CB(2) agonists using parallel synthesis protocols: A Lipophilic Efficiency (LipE) analysis. *Bioorg. Med. Chem. Lett.* **2009,** *19*, 4406-4409.

37. Saal, C.; Petereit, A. C. Optimizing solubility: kinetic versus thermodynamic solubility temptations and risks. *Eur. J. Pharm. Sci.* **2012,** *47*, 589-595.

38. Copeland, R. A.; Basavapathruni, A.; Moyer, M.; Scott, M. P. Impact of enzyme concentration and residence time on apparent activity recovery in jump dilution analysis. *Anal. Biochem.* **2011,** *416*, 206-210.

39. Van Aller, G. S.; Pappalardi, M. B.; Ott, H. M.; Diaz, E.; Brandt, M.; Schwartz, B. J.; Miller, W. H.; Dhanak, D.; McCabe, M. T.; Verma, S. K.; Creasy, C. L.; Tummino, P. J.; Kruger, R. G. Long residence time inhibition of EZH2 in activated polycomb repressive complex 2. *ACS Chem. Biol.* **2014,** *9*, 622-629.

40. Beguelin, W.; Popovic, R.; Teater, M.; Jiang, Y.; Bunting, K. L.; Rosen, M.; Shen, H.; Yang, S. N.; Wang, L.; Ezponda, T.; Martinez-Garcia, E.; Zhang, H.; Zheng, Y.; Verma, S. K.; McCabe, M. T.; Ott, H. M.; Van Aller, G. S.; Kruger, R. G.; Liu, Y.; McHugh, C.

F.; Scott, D. W.; Chung, Y. R.; Kelleher, N.; Shaknovich, R.; Creasy, C. L.; Gascoyne, R. D.; Wong, K. K.; Cerchietti, L.; Levine, R. L.; Abdel-Wahab, O.; Licht, J. D.; Elemento, O.; Melnick, A. M. EZH2 is required for germinal center formation and somatic EZH2 mutations promote lymphoid transformation. *Cancer Cell* **2013,** *23*, 677-692.

41. The high exposures are likely due to saturation of clearance.
42. Edwards, M. P.; Kumpf, R. A.; Kung, P.-P.; McAlpine, I. J.; Ninkovic, S.; Rui, Eugene Y.; Sutton, S. C.; Tatlock, J. H.; Wythes, M. J.; Zehnder, L. R. Aryl and heteroaryl fused lactams. WO 2014/097041 A1, June 26, 2014.
43. Ghosh, A. K.; Thompson, W. J.; Holloway, M. K.; McKee, S. P.; Duong, T. T.; Lee, H. Y.; Munson, P. M.; Smith, A. M.; Wai, J. M.; Darke, P. L.; Zugay, J. A.; Emini, E. A.; Schleif, W. A.; Huff, J. R.; Anderson, P. S. Potent HIV protease inhibitors: the development of tetrahydrofuranylglycines as novel P2-ligands and pyrazine amides as P3-ligands. *J. Med. Chem.* **1993,** *36*, 2300-2310.
44. Khurana, J. M. and Kukreja, G. Rapid reduction of nitriles to primary amines with nickel boride at ambient temperature. *Synth. Commun.* **2002**, *32*, 1265-1269.
45. Kurouchi, H.; Sumita, A.; Otani, Y.; and Ohwada, T. Protonation switching to the least-basic heteroatom of carbamate through cationic hydrogen bonding promotes the formation of isocyanate cations. *Chem. - Eur. J.* **2014**, *20*, 8682-8690.
46. Compound **1** was purchased from Active Biochem.

Figure 1. Literature reported EZH2 inhibitors

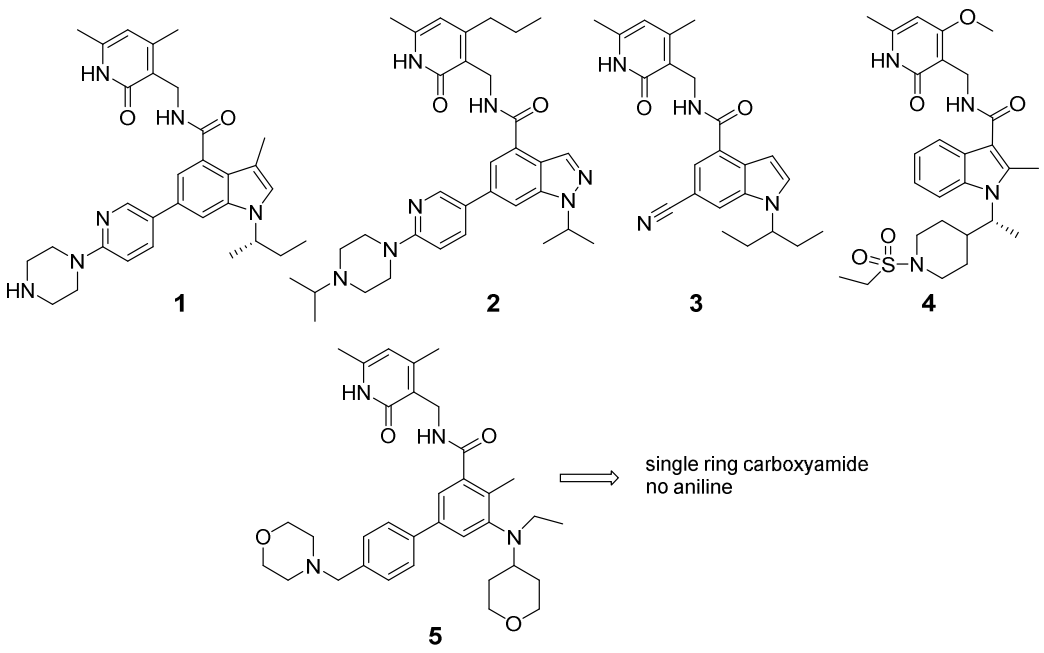

Figure 2. A carboxyamide library contains dimethylpyridone moiety

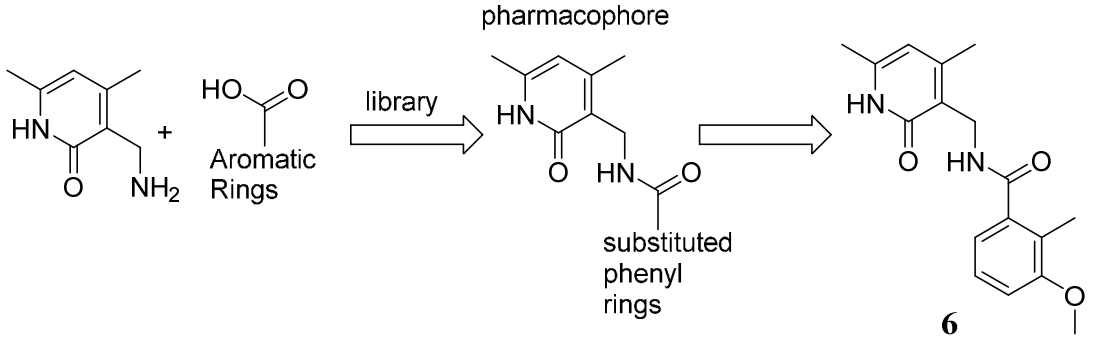

Table 1. Structure activity relationship of R^1 and R^2 substituents

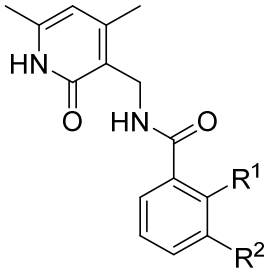

Compound#	R^1	R^2	Bio WT IC_{50} (μM)[a]	logD[b]	LipE (Bio WT)
6	**CH_3**	**OCH_3**	5.7	1.5	3.7
7	**CH_3**	**H**	>200	1.4	
8	**H**	**OCH_3**	>150	1.7	
9	**CH_3**	**OCH_2CH_3**	2.0	2.1	3.6
10	**CH_3**	**$OCH(CH_3)_2$**	1.4	2.1	3.8
11	**F**	**OCH_3**	>150	1.4	
12	**OCH_3**	**OCH_3**	>140	1.7	
13	**OH**	**OCH_3**	44	1.9	2.5
14	**Cl**	**OCH_3**	7.2	1.2	4.0
15	**Cl**	**$OCH(CH_3)_2$**	1.3	2.0	3.9

[a]values were determined from 11-point dose response curves in duplicate. All compounds were tested in at least two independent experiments with most compounds being tested three or four times, some more than four times. The values shown are geometric means of the replicates. In most cases, all individual replicates are within 2-fold of each other
[b]logD was measured at pH 7.4.

Figure 3. Distribution of the observed relative fractions of the CCC=O torsion angle in the CSD database for various R^1 substituted Benzamides

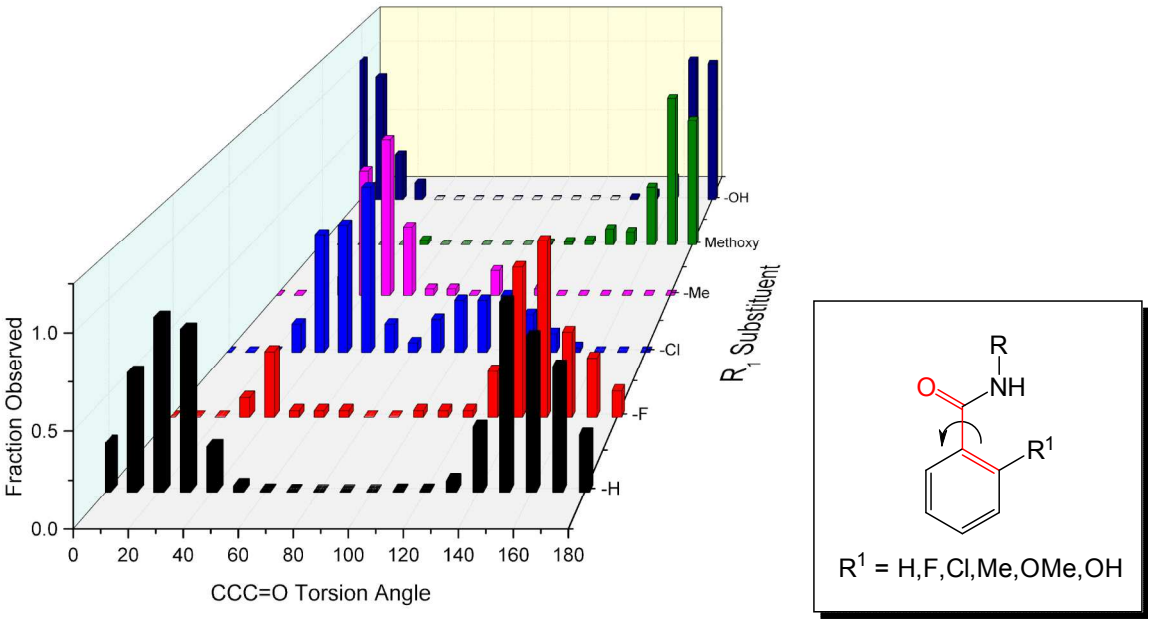

Table 2. Cyclization of benzamide 14 to form 7-membered ring and 6-membered ring lactam (11-13)

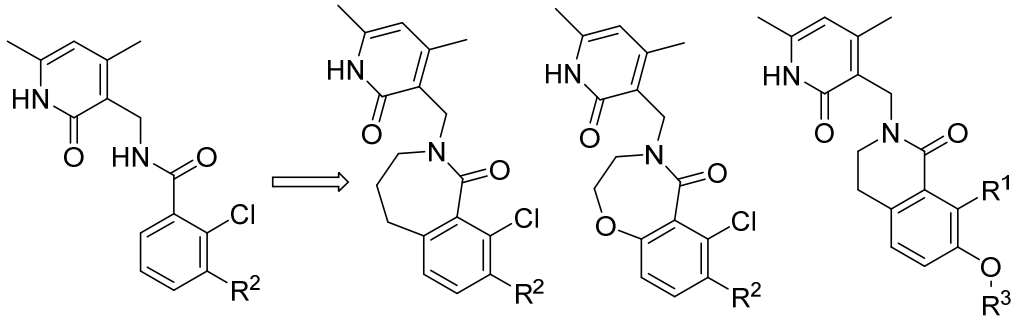

14, R^2 = OMe **16,** R^2 = OMe **17,** R^2 = OMe

18, R^1=Cl; R^3 = Me
19, R^1=Cl; R^3 = Et
20, R^1=Cl; R^3 = isopropyl
21, R^1=CH_3; R^3 = isopropyl
22, R^1=H; R^3 = isopropyl

Compound no.	Bio WT IC_{50} (μM)[a]	HLM Cl (μL/min/mg)	logD[b]	LipE (Bio WT)
14	7.2	8	1.2	4.0
16	0.15	82	1.7	5.2
17	0.65	40	1.3	4.9
18	0.35	35	1.8	4.7
19	0.13	37	2.2	4.7
20	0.041	53	2.7	4.7

21	0.16	102	2.9	3.9
22	8.1	19	2.5	2.6

[a]values were determined from 11-point dose response curves in duplicate. All compounds were tested in at least two independent experiments with most compounds being tested three or four times, some more than four times. The values shown are geometric means of the replicates. In most cases, all individual replicates are within 2-fold of each other
[b]logD was measured at pH 7.4.

Table 3. Isothermal titration calorimetry results for compounds 10 and 21

Compound#	n	K_d (nM)	ΔG (kcal mol^{-1})	ΔH (kcal mol^{-1})	-TΔS (kcal mol^{-1})
10	0.73 ± 0.10	252 ± 36	-8.85	-7.30 ± 0.54	-1.55
21	0.81 ± 0.05	37.4 ± 4.8	-9.96	-6.06 ± 0.38	-3.90

Equilibrium dissociation constant (K_d), binding stoichiometry (n), and enthalpy change (ΔH) were measured by ITC.
Free energy change (ΔG) and entropy change (ΔS) were calculated from the K_d and ΔH at 20 ^oC.
Standard deviations were determined from triplicate experiments.

Figure 4. Molecular pair comparison of potency and LipE for lactam analogs vs. benzamide analogs

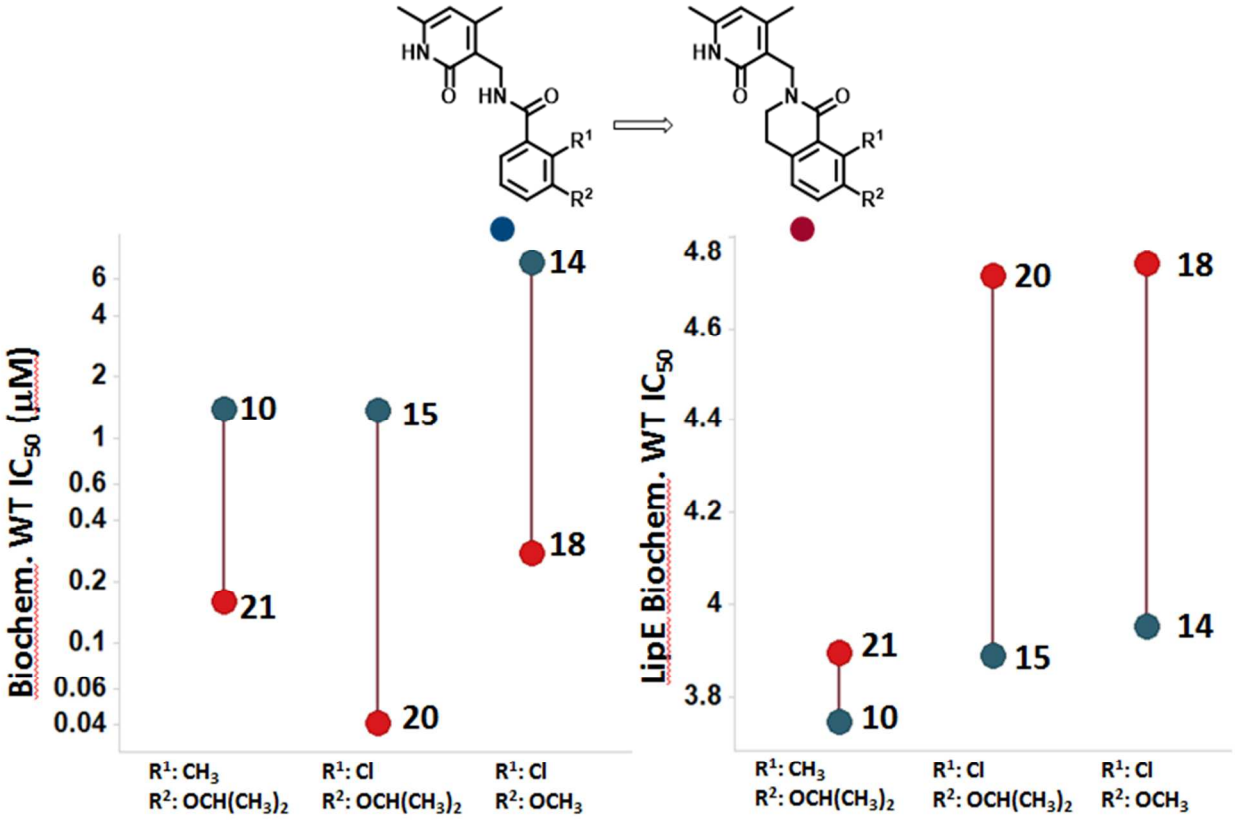

Table 4. Structure activity relationship of R^2 and R^4 substituents

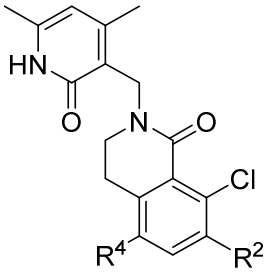

Compound#	R^2	R^4	WT IC_{50} (nM)[a]	Y641N IC_{50} (nM)[a]	logD[b]	H3K27me3 IC_{50} (nM)	Proliferation IC_{50} (nM)
20	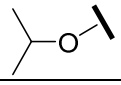	**H**	41	160	2.7	1187	1155
23	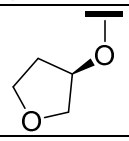	**H**	28	110	1.5	796	512
24	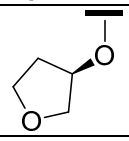	**F**	56	260	2.1	994	1026
25	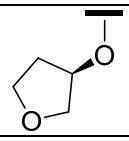	**CH_3**	18	61	2.1	290	406
26	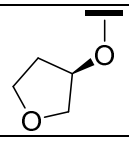	**Cl**	5.6	18	2.5	170	155
27	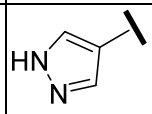	**Cl**	51	270	3.0	1726	1580

28	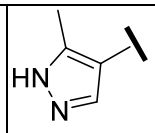	**Cl**	24	110	3.1	873	1336
29	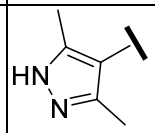	**Cl**	16	82	3.4	502	959
30	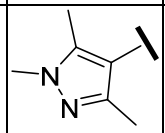	**Cl**	1500	6000	3.4	15308	12757
31	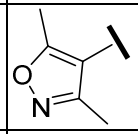	**Cl**	0.7*	3.0*	3.1	15	25
32	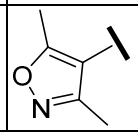	**H**	3.2 2.0*	8.8 6.3*	2.6	105	121

[a]values were determined from 11-point dose response curves in duplicate. All compounds were tested in at least two independent experiments with most compounds being tested three or four times, some more than four times. The values shown are geometric means of the replicates. In most cases, all individual replicates are within 2-fold of each other

*Ki value was determined using the method described in the supplementary material. IC_{50} values for compound **31** could not be accurately determined under the assay conditions due to the high potency of the compound.

[b]logD was measured at pH 7.4.

Figure 5. LipE comparison for compounds 6, 9, 10, 13, 14-32[a]

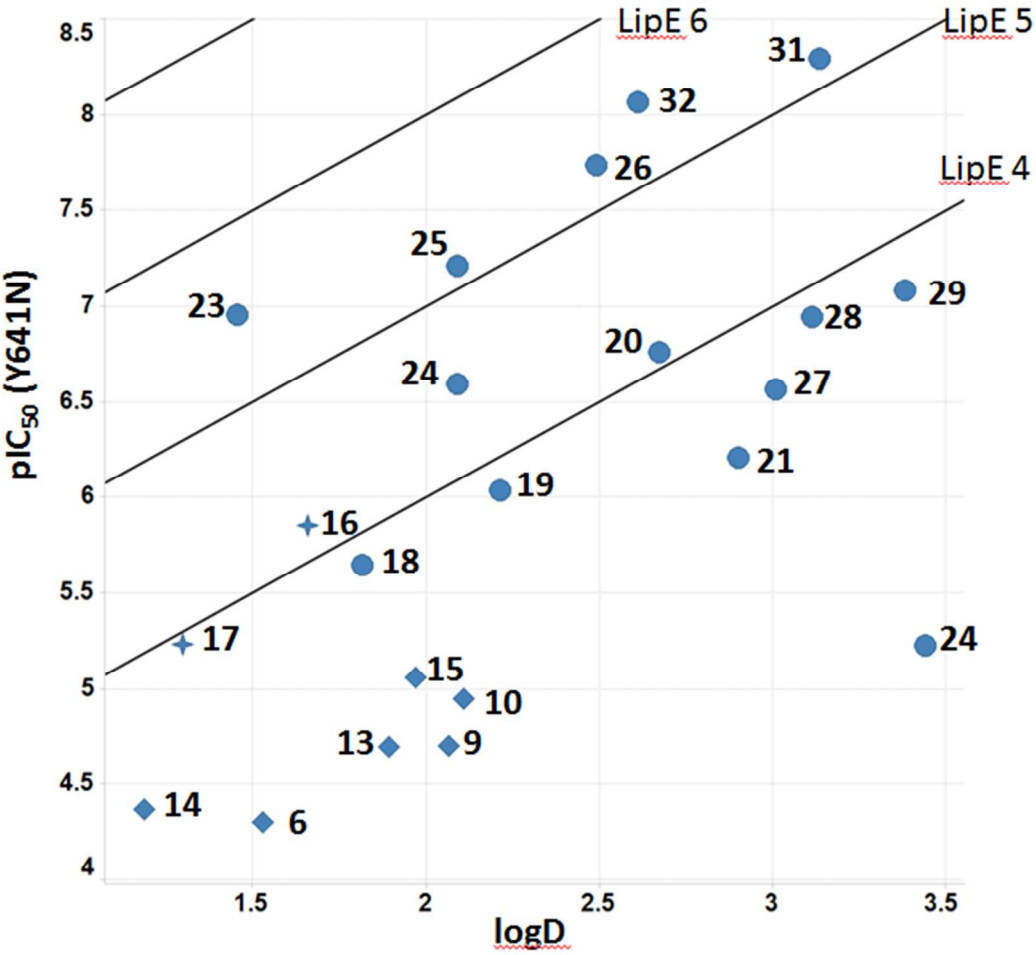

[a]compounds **7**, **8**, **11**, **12** are not shown in the spotfire plot due to week potency in Y641N biochemical assay.
diamond shape: benzamide
circle shape: 6-membered lactam
star shape: 7-membered lactam

Table 5. ***In vitro*** **ADME and physical properties for selective EZH2 inhibitors**

Compound#	Microsomal stability (μL/min/mg)		RRCK permeability ($X10^{-6}$/sec)	MDCK/MDR1 permeability ($X10^{-6}$/sec)		Solubility (μM)
	human	mouse		AB	BA/AB	
20	53.8	ND	19.6	7.9	2.2	19.6
23	21	31	12.3	1.7	8.6	510
26	21	163	14.7	4.5	4.7	26
31	107	531	15.7	5.2	4.6	93.5

Figure 6. Mouse free[a] plasma exposure for compound 31 relative to cellular IC_{90}/IC_{50} value

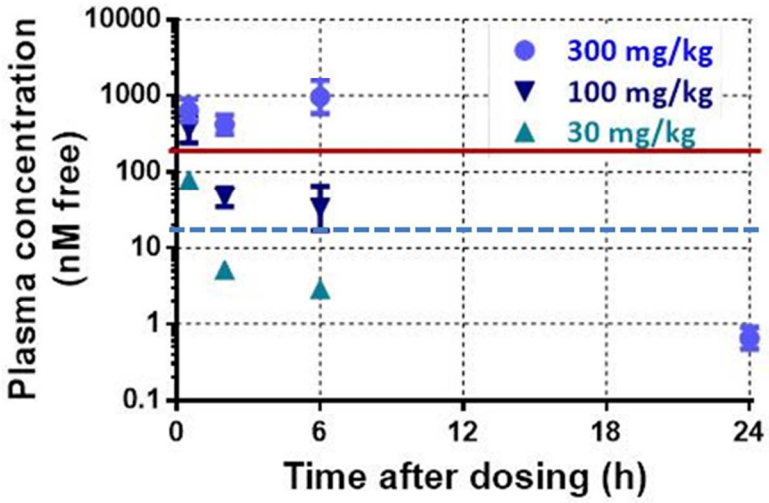

[a]Mouse plasma protein binding: 15%
red solid line and blue dotted line indicated *in vitro* IC_{90} and IC_{50} values, respectively, from cellular readout

Figure 7. Compound 31 inhibits tumor growth and induces robust modulation of downstream biomarkers in a Karpas-422 in vivo model.

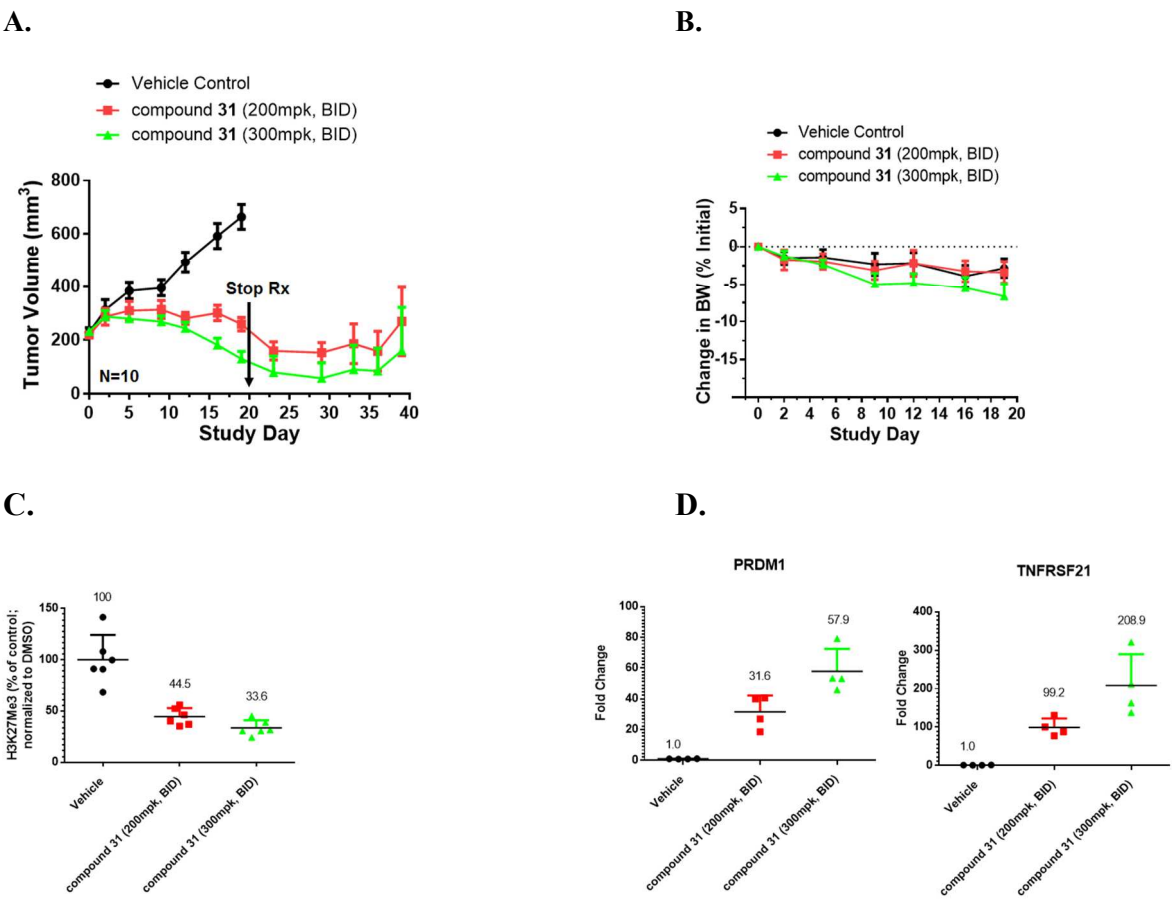

A) Tumor growth inhibition in a subcutaneous Karpas-422 xenograft model. Mice were treated with Compound 31 at 200mpk and 300mpk BID for 20 days. Tumor growth was monitored for several weeks following cessation of dosing. B) Average body weight measurements during the duration of compound treatment. C) Measurement of golbal H3K27Me3 levels in Karpas-422 tumors harvested on day 20. D) Expression of PRC2 target genes, PRDM1/TNFRSF21, following 20 days of treatment with compound 31.

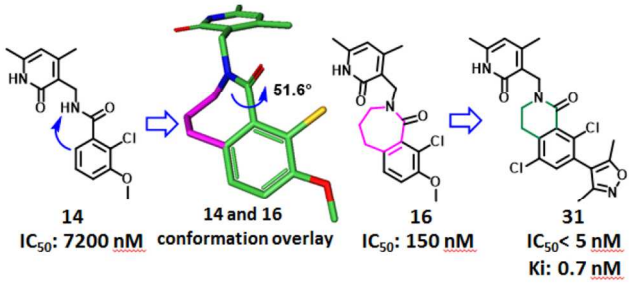

Table of Contents graphic
Table of Contents graphic
254x190mm (150 x 150 DPI)